



MINISTRY OF AVIATION  
AERONAUTICAL RESEARCH COUNCIL  
CURRENT PAPERS

# Measurements of Pressure Fluctuations on the Surface of a Delta Wing

By

*V. Krishnamoorthy*

LONDON: HER MAJESTY'S STATIONERY OFFICE

1965

SIX SHILLINGS NET



MEASUREMENTS OF PRESSURE FLUCTUATIONS  
ON THE SURFACE OF A DELTA WING

August, 1963

by

V. Krishnamoorthy

SUMMARY

Measurements have been made of the r.m.s. levels, spectra and space correlations of the surface pressure fluctuations on a  $76^\circ$  sharp edged delta wing at low incidences. The peak r.m.s. value was found to be 3.7 times that for the  $0^\circ$  incidence and occurred under the main vortex at  $2^\circ$  incidence. The forms of the spectra were found to be not dissimilar to that for  $0^\circ$  incidence. This suggests that the fluctuations arise from the boundary layer modified by the vortex. The correlation radius was found to be about  $\frac{1}{15}$ th of the local semi-span. However, correlation lengths for discrete frequencies could be twice as large as this.

List of Contents

	<u>Page No.</u>
Summary	
1. Introduction .. .. .	1
2. Experimental Apparatus .. .. .	1
3. Discussion of Experiments and Results .. .. .	2
3.1 The Nature of the Boundary Layer used in the Investigation .. .. .	2
3.2 Measurements of the R.M.S. Value of Fluctuating Pressures on the Wing .. .. .	2 & 3
3.3 Frequency Spectra of the Pressure Fluctuations .. .. .	3, 4 & 5
3.4 Space Correlation Measurements of the Pressure Fluctuations .. .. .	5, 6 & 7
4. Conclusions .. .. .	7
Acknowledgements .. .. .	7
List of Symbols .. .. .	8 & 9
References .. .. .	10
Figures 1-18	



## 1. Introduction

Experiments by T. B. Owen of R.A.E. (unpublished) on a slender delta wing with sharp leading edges showed that appreciable pressure fluctuations were present on the upper surface at low incidences. There was a characteristic increase in the intensity of pressure fluctuations immediately beneath the vortex and also in the region between the secondary separation line and the leading edge. For low Mach numbers a peak value of about three times the two-dimensional turbulent boundary layer of r.m.s. pressure fluctuations occurred at an angle of incidence of  $2^\circ$ . It was also found that the amplitude of these pressure fluctuations depended on Reynolds number and the method of fixing transition.

The unsteady loading due to the leading-edge vortex and the effects of the boundary-layer noise are of great interest from the fatigue point of view. The response of an aeroplane and its structures to these pressures depends upon the space correlations as well as intensity levels and frequency spectra. The only surface pressure correlation measurements so far reported were made by Judd and Jones<sup>1</sup> and they covered a wide incidence range starting from  $12^\circ$  up to the vortex breakdown.

The present investigation was undertaken to determine more accurately the levels and frequency spectra of the fluctuating pressures at the wing surface and to find the correlation areas of the pressures particularly at low incidence.

## 2. Experimental Apparatus

Measurements were made on a  $76^\circ$  delta wing in the University of Southampton  $7\frac{1}{2}$  ft  $\times$   $5\frac{1}{2}$  ft wind tunnel. The turbulence of the axial velocity component was measured to be  $\sqrt{u'^2}/U_\infty \simeq 8 \times 10^{-4}$ . The model was a sharp edged flat plate wing with a chamfered under-surface. Hypodermic tubes of 0.049 in. outside diameter were inserted flush with the upper-surface of the wing but projecting on the under-side. The distribution of the pressure tappings is shown in Figs. 1 and 2. The fluctuating pressures at the tappings were detected using two matched probe microphones butt-connected to the projection and sealed by plastic sleeves. The microphone dimensions and construction are described by Franklin and Archbold<sup>2</sup> and they were built around a one inch Bruel and Kjaer condenser capsule type 4111.

The probes were calibrated by comparing their outputs with that of a calibrated standard Bruel and Kjaer microphone when subjected to the same noise source - in this case a loud speaker in an anechoic chamber. The loud speaker was fed from a white noise generator. The signals from the transducers were fed to the main microphone amplifiers, which had a gain characteristic rising at +6dB per octave to compensate for the fall in response of the probes, via pre-amplifiers. The sensitivities of the transducers were found to be  $11.48$  mv/ $\mu$  bar and  $14.10$  mv/ $\mu$  bar respectively with full gain on. Attenuation of gain was possible in steps of 10dB. The frequency response of the probe and microphone amplifier combination was very nearly flat from 50 c/s to 3 000 c/s. The capsules of the transducers were designed to work in a region of atmospheric static pressure but tests showed that there was negligible effect on their calibrations at the tunnel speeds used.

The root-mean-square measurements of the pressure fluctuations were made by a Dawe type true r.m.s. meter. For spectral density measurements, the amplified signals from the pressure transducers were recorded on a Vortexion

tape recorder which had a near flat frequency response up to 15 Kc/s. The recorded signal was analysed by a Muirhead Pamatrada narrow band wave analyser which covered a frequency range of 20 c/s to 20 Kc/s. The effective band width of the analyser was 0.048 times the mid-band width frequency.

For correlation measurements, the fluctuating pressures at various points on the wing surface were recorded on a twin-channel magnetic tape recorder. The recorder was calibrated and it was established that recording and replaying of the signals introduced no time delay in the two channels.<sup>3</sup> The records were later analysed in the University of Southampton correlator<sup>3</sup>. This is an analogue computer and calculates space, auto and cross-correlation coefficients between any pair of signals. The correlator was calibrated by forming the auto-correlation of sine waves.

### 3. Discussion of Experiments and Results

#### 3.1 The nature of the boundary layer used in the investigation

The first problem was to ensure that the boundary layer over the wing was fully turbulent, as would be the case for a full-scale wing. The majority of the tests were conducted at a speed of 110 ft/sec. and the Reynolds number based on the wing root chord was  $2.2 \times 10^6$ . Since natural transition was occurring over parts of the wing at this Reynolds number, the boundary layer was tripped by applying distributed roughness at the apex of the wing. Carborundum Powder (grade 60) was applied at the leading edges up to 5% chord. Flow visualisation experiments using the technique<sup>4</sup> of Saturn Yellow pigment and Ultra-violet light confirmed that the boundary layer was turbulent over the wing for the incidences required. Figs. 3 and 4 show the flow pattern over the wing without and with roughness at the apex. Without roughness transition occurred as far back as 35% of the root chord at an incidence of  $15.5^\circ$ . There are pronounced kinks in the secondary separation line suggesting that transition disturbs only the secondary region but not the main vortex flow pattern. With roughness on, the transition point moved forward and occurred at some point close to the apex, the precise location of which was a function of the model incidence.

The effect of roughness on the spanwise static pressure distribution for the front station ( $x/c_0 = 0.333$ ) is shown in Fig. 5. When there is no roughness, a marked double peak corresponding to the main and secondary vortices is found. With roughness, the suction peak under the main vortex increases and the secondary peak tends to become flat. For the rear station ( $x/c_0 = 0.666$ ) at all incidences, the pressure distribution was unaffected by roughness since transition had already occurred upstream.

#### 3.2 Measurements of the r.m.s. values of the fluctuating pressures on the wing

The results for the r.m.s. pressure fluctuations measured across the wing at various incidences are shown in Figs. 6 and 7 for the two chord-wise positions. Roughness was used and the results are presented as  $\sqrt{p^2}/q_\infty$  against spanwise position. The pressure tappings were at close intervals extending as close as practicable to the leading edge.

For/

For the front station, it is seen from Fig. 6 that at  $0^\circ$  incidence the value of  $\sqrt{p^2}/q_\infty$  was 0.0066 and remained constant up to  $y/s = 0.75$ . There was a gradual increase then in level towards the leading edge. This might be due to the local skin friction coefficient which is a function of the local Reynolds number being higher outboard than for the inboard tappings. Alternatively the wing may not have been at a true  $0^\circ$  incidence. At  $2^\circ$  incidence, there was a large rise in pressure fluctuation level and two peaks were observed between the attachment line and the leading edge. These peaks are probably caused by the main and secondary vortices. The absolute peak value reached was  $\sqrt{p^2}/q_\infty = 0.0198$ , three times the  $0^\circ$  value. With increase in incidence the curves broadened with reduced peak values. The main peak moved inwards, but the secondary peak appeared to settle at  $y/s = 0.81$  at  $6^\circ$  and beyond this angle there was very little movement. The trough between the peaks became more pronounced at higher incidences. This is probably because the tappings lie just under the outboard edge of the main vortex. There was better agreement in correlating the main peak r.m.s. level with the point of inflexion of the flow visualisation and static spanwise pressure distribution tests - than for correlating the secondary peak with the secondary separation line.

Fig. 7 shows that at  $0^\circ$ ,  $\sqrt{p^2}/q_\infty = 0.0068$  for the rear station and remains constant up to  $y/s = 0.79$  and then increases at the outer tappings. At  $2^\circ$  incidence the peak r.m.s. was 0.0252, 3.7 times the  $0^\circ$  value. As before, the two peak levels corresponding to the main and secondary vortices decrease with increasing incidence. The inward movement of the main peak followed the points of inflexion of the stream lines of the main vortex but the secondary peak had only fair agreement with the secondary separation line as seen from the flow visualization tests. At  $8^\circ$ , the peak  $\sqrt{p^2}/q_\infty$  had a value slightly higher than twice the  $0^\circ$  level.

To determine the effect of roughness on the fluctuation levels, tests were conducted with no roughness at the apex. The r.m.s. values across the vortex are shown in Fig. 8 for the front station at two angles of incidence. The values in the secondary separation region show a much higher level without roughness than with roughness on.

### 3.3 Frequency spectra of the pressure fluctuations

The fluctuating pressure on a flat plate is assumed to be a stationary random function of time  $t$  and position  $x, z$ . The  $x$  and  $z$  axes lie in the plane of the plate, with  $x$  increasing in the stream direction. Using the properties of stationary random functions, the correlation or covariance of the pressure is

$$R_{pp}(x_1, x_2, \tau) = \frac{\overline{p(x, z, t) p(x+x_1, z+z_2, t+\tau)}}{\sqrt{\overline{p^2(x, z, t)} \overline{p^2(x+x_1, z+z_2, t+\tau)}}} \dots (1)$$

and/

and the Fourier transform of the auto-correlation of the pressure is defined by

$$\overline{p^2} R_{pp}(0,0,\tau) = \int_0^\infty E(\omega) \cos \omega\tau \, d\omega. \quad \dots(2)$$

The inverse is 
$$E(\omega) = \frac{1}{\pi} \int_0^\infty \overline{p^2} R_{pp}(0,0,\tau) \cos \omega\tau \, d\tau. \quad \dots(3)$$

$E(\omega)$  is the power spectral density of the pressure fluctuation as measured by a wave analyser.

The spectral measurements were made with the same probe microphones as were used for the r.m.s. measurements. At  $0^\circ$  incidence the spectra were measured at the centre line of the wing at the front and rear stations with roughness fixed at the apex. Since there was no flow separation at the leading edge and the flow direction remained chordwise everywhere the boundary layer on the wing could be approximated to a two-dimensional turbulent boundary layer growing on a flat plate.

The power spectrum of the delta wing at  $0^\circ$  incidence is shown in dimensionless form in Fig. 9. The velocity profiles were measured at both stations and the displacement thicknesses calculated. The tests covered a frequency range of  $0.0136 < \frac{\omega\delta^*}{U_\infty} < 0.816$ . Frequencies higher than this could not be covered because of the limitations of the transducer frequency response characteristics. But it is seen that this range sweeps the main energy content in the spectrum. When the power spectra of the wing are compared with the wall pressure spectrum of Willmarth and Wooldridge<sup>5</sup> in Fig. 9, it is found that the wing spectra are fairly flat at low frequencies but higher in levels than that of Willmarth. Willmarth's measurements were made in a thick boundary layer developed on a smooth surface with natural transition. On a rough plate Willmarth found the r.m.s. levels to be 0.007 and 0.0066 for two wind speeds as against 0.00466 for the smooth wall. Hence the spectrum levels for the rough condition should be higher than the wall power spectrum of Fig. 9. At the upper end of the frequency spectra, the levels for the delta wing tend to fall more rapidly than the wall pressure levels. This may be due to the fall off in sensitivity of the probes at higher frequencies.

The spectral measurements were taken on different occasions and found repeatable. A series of tests were conducted to find the effect on the pressure transducers of extraneous signals such as the sound field in the test section and the support vibrations. To determine the effectiveness of the mounting, the probes were sealed from the boundary-layer pressure fluctuations while the wind was on. The signals produced by the vibration of the mounting amounted to 1% of the r.m.s. wall pressure fluctuations.

To determine the noise level inside the tunnel a Bruel and Kjaer  $\frac{1}{2}$  in. diameter microphone was installed in a bullet shaped wind shield. The shield had a band of fine gauze placed along the parallel portion so that the wind was not directly onto the diaphragm. The microphone was facing downstream with its diaphragm normal to the flow. The spectrum of the sound field was measured in a frequency band of 50 c/s to 10 000 c/s with a Bruel and Kjaer  $\frac{1}{3}$  octave analyser. It is likely that below 300 c/s the spectra of the surface pressure fluctuations are increased by the tunnel noise; the main sources of the tunnel noise were the driving fan and the tunnel wall boundary layer.

The power spectra  $E(f)$  of the pressure fluctuations for various incidences are shown as a function of frequency in Figs. 10 and 11 for the front and rear stations with roughness on. Most of the spectra were measured at span-wise positions corresponding to the peak r.m.s. levels. The measuring points are shown in the figures. The spectra could not be presented in a dimensionless form because of the three-dimensional nature of the flow the value  $U/\delta^*$  could not be established. At the incidences other than  $0^\circ$ , a leading-edge vortex was formed and mixed with the boundary layer. The technique used by Owen<sup>6</sup> of presenting the spectra in a non-dimensional form using wing root chord instead of displacement thickness for the frequency parameter is not used here. Owen's method has greater utility in examining buffeting excitations. It was thought that the present form of plotting the spectra could throw more light on the effect of the vortex on the pressure fluctuations on the wing. The  $0^\circ$  plots correspond to the spectra presented in dimensionless form in Fig. 9. At other incidences the highest levels occur near 100 c/s and most of the energy in the spectrum is contained below 2 000 c/s.

At incidence apart from the pressure rise and increased energy levels, the shapes of the spectra are not very different from those of the  $0^\circ$  incidence pressure fluctuations. Therefore it seems possible that the pressure fluctuations arise from the boundary layer on the wing. The differences in spectra can probably be accounted for by the modification of the boundary-layer characteristics by the vortex in increasing the local free stream velocity reducing the thickness of the boundary layer and forming pressure gradients.

It appears that further measurements ought to be made to determine the mean velocities through the boundary layer and the vortex to know the extent of interaction of the vortex with the boundary layer. Since the intensity of pressure fluctuations reaches a maximum at  $2^\circ$  incidence, it is possible that the boundary layer and the vortex are merged leaving no clear distinction between them at this incidence.

### 3.4 Space correlation measurements of the pressure fluctuations

Twin channel magnetic tape recordings of fluctuating pressures were made for the two rosettes at incidences  $0^\circ$ ,  $2^\circ$ ,  $3^\circ$ ,  $4^\circ$ ,  $6^\circ$ ,  $8^\circ$  and  $9^\circ$ . The measurements were taken from the output of the microphones and simultaneous tape recordings were made with one microphone fixed at the rosette centre tapping and the second at other points in between.

From/

From the recordings the distribution of space correlation coefficient  $R_s$  and filtered space correlation coefficient  $R_{sn}$  were obtained. The above correlation coefficients are defined as

$$R_s = \lim_{T \rightarrow \infty} \frac{1}{2T} \int_{-T}^T \frac{f_a(t) f_b(t)}{F_a F_b} dt \quad \dots(4)$$

$$R_{sn} = \lim_{T \rightarrow \infty} \frac{1}{2T} \int_{-T}^T \frac{f_{an}(t) f_{bn}(t)}{F_{an} F_{ab}} dt. \quad \dots(5)$$

The integration time  $T$  used in practice was 20 seconds.

The correlation length and correlation area used in the discussion are quite arbitrary. The correlation length is defined to be the distance from a reference point over which the space correlation coefficient,  $R_s$ , has a value greater than +0.4 with respect to the signal at the reference point. The correlation area is similarly defined as the area over which  $R_s$  is greater than 0.4 with respect to the reference signal. The accuracy of the correlation technique is such that values of  $R_s$  less than about 0.1 and minor fluctuations of  $R_s$  can not be regarded as significant.

The directional variation of the overall space correlation coefficient is shown in Fig. 12 for the forward rosette. At 0°, the correlation coefficient around the inner ring is a maximum in the East-West direction. Around the outer ring a maximum correlation coefficient of 0.5 is reached in the Southern direction, but in all other directions the correlation coefficient in this context is too small to be considered.

The effect of increasing the incidence is to increase the correlation area and to smooth out the variations with the azimuth. From Fig. 13 it is seen that in the rear rosette, at 0° incidence the variation of  $R_s$  is similar to that for 0° in the front rosette. At 3°, the variations are smoothed and this trend continues for higher incidences as well. It appears that the inner ring of points forms the boundary for both the rosettes.

The variation of correlation coefficient in the N.W. - S.E. diagonal with changing incidence is shown in Figs. 14 and 15 for the two rosettes. Ignoring coefficients of less than 0.4, it is seen that increasing the incidence from 0° to 6° causes minor increase in correlation area. The correlation radius is about  $\frac{1}{15}$  th of the local semi-span for both the rosettes.

The space correlation along this diagonal for various frequency bands from 200 c/s to 1 000 c/s is shown in Figs. 16 and 17. It can be seen that the fluctuations are well correlated over a larger radius at low frequencies.

The/

The effect of roughness on the variation of correlation coefficient for the forward rosette is shown in Fig. 18. At  $4^\circ$  the correlation coefficients have the same value for the no roughness and roughness on conditions. At higher angles there is a decrease in the values and also the correlation radius is reduced, but not significantly, for the no roughness case.

#### 4. Conclusions

1. R.M.S. levels, frequency spectra and space correlation measurements were obtained using a pair of probe microphones. The corrected r.m.s. level of the boundary-layer pressure fluctuations at zero degree incidence was found to be 0.0066 and 0.0068 respectively for the two chordwise stations on the wing.

2. The r.m.s. levels across the wing were found to increase at incidence due to the formation of the vortex. Two peaks were observed one under the main vortex and the other in the secondary separation region. The highest level was reached at  $2^\circ$  and was found to be  $\sqrt{p^2}/q_\infty = 0.0252$  (3.7 times the  $0^\circ$  level), at the rear station underneath the main vortex. The peak value reached at the front station for the same angle was 0.0198 (3 times the  $0^\circ$  level). These values apply when roughness was used and the flow was turbulent everywhere.

3. Further increase in incidence indicates a fall in peak levels at the two stations, though still higher than the  $0^\circ$  level.

4. Roughness has little influence on the r.m.s. levels of the main vortex. The r.m.s. levels in the secondary separation region are higher without roughness. The degree of roughness used has no influence on the levels provided the flow is made sufficiently turbulent.

5. Most of the energy is contained in the low frequency range of the spectra. The peak values occur near 100 c/s. The form of the spectra at incidence apart from the pressure rise and higher energy levels is not dissimilar to the  $0^\circ$  case.

6. The correlation radius is found to be about  $\frac{1}{15}$ th of the local semi-span for the two stations. The fluctuations are well correlated over  $\frac{1}{7}$ th of the semi-span at lower frequencies.

The origin of the pressure fluctuations at low incidences seems to be a boundary-layer phenomenon. Lilley<sup>7,8</sup> following from his work on two-dimensional turbulent boundary-layer pressure fluctuations suggested that at points on the wing surface there should be a linear relationship between the r.m.s. amplitude of the local pressure fluctuations and the local surface shear stress. Wyatt and Owen<sup>9</sup> have confirmed this in some recent experiments.

#### Acknowledgements

My thanks are due to Dr. J. P. Jones and Dr. M. Judd for their encouragement in this work and to the Commonwealth Scholarship Commission for a financial award to enable me to stay in England.

List of Symbols/

List of Symbols

$c_o$	root chord of the wing.
$C_p$	static pressure coefficient.
$E(\omega)$	power spectrum of static pressure.
$f$	frequency.
$f_a$	randomly varying signal at position a.
$f_{an}$	resultant signal after filtering $f_a$ at a particular frequency.
$f_b$	randomly varying signal at position b ( $=a + a^1$ )
$a^1$	spatial separation between the two measuring points.
$f_{bn}$	resultant signal after filtering $f_b$ at a particular frequency.
$F_a$	r.m.s. level of $f_a$ .
$F_{an}$	r.m.s. level of $f_{an}$ .
$F_b$	r.m.s. level of $f_b$ .
$F_{bn}$	r.m.s. level of $f_{bn}$ .
$p$	static pressure.
$\sqrt{p^2}$	r.m.s. level of the pressure fluctuation.
$q_{\infty}$	free stream dynamic pressure.
$r$	radial distance measured from the rosette centre.
$R_{pp}$	normalized pressure correlation coefficient.
$R_s$	overall space correlation coefficient.
$R_{sn}$	filtered space correlation coefficient.
$Re$	Reynolds number.
$s$	local semi-span.
$t$	time.
$T$	integration time.
$\tau$	time delay.
$U_{\infty}$	free stream velocity.
$U_o$	velocity at the edge of the boundary-layer.

- $\sqrt{u'^2}$  r.m.s. axial velocity component of the free stream turbulence.
- $\omega$  angular frequency.
- $x$  chordwise co-ordinate.
- $y$  spanwise co-ordinate.
- $z$  spanwise distance in the case of flat plate.
- $x_1, x_3$  spatial separation of pressure transducers in x or z direction for the flat plate.
- $\alpha$  angle of incidence of the model.
- $\delta^*$  displacement thickness of the boundary-layer.
- 

References/

References

<u>No.</u>	<u>Author(s)</u>	<u>Title, etc.</u>
1	M. Judd and J. P. Jones	Surface Pressure Fluctuation Correlation Measurements on a 70° Delta Wing. A.R.C.22 428. December, 1960.
2	R. E. Franklin and R. B. Archbold	A Small-Bore Pick-Up for the Measurement of Fluctuating Pressure. The Aeronautical Quarterly, Vol.XI. November, 1960.
3	G. A. Allcock, P. L. Tanner and K. R. McLachlan	A General Purpose Analogue Computer for the Analysis of Random Noise Signals. University of Southampton Report. A.A.S.U.205.
4	R. L. Maltby and R. F. A. Keating	Flow Visualisation in Low-Speed Wind Tunnels: Current British Practice. R.A.E. Tech. Note AERO 2715. A.R.C.22 373. August, 1960.
5	W. W. Willmarth and C. E. Wooldridge	Measurements of the Fluctuating Pressure at the wall beneath a thick Turbulent Boundary Layer. Journal of Fluid Mechanics. Vol. 14, pp 187-210. 1962.
6	T. B. Owen	Techniques of Pressure Fluctuation Measurements Employed in the R.A.E. Low-Speed Wind-Tunnels. AGARD Report 172. March, 1958.
7	G. M. Lilley and T. H. Hodgson	On the Surface Pressure Fluctuations in Turbulent Boundary Layers. AGARD Report 276. 1960.
8	G. M. Lilley	Pressure Fluctuations in an Incompressible Turbulent Boundary Layer. College of Aeronautics, Cranfield. Report No. 133. 1960. A.R.C.22 019. June, 1960.
9	L. A. Wyatt and T. B. Owen	Preliminary Low-Speed Measurements of Skin-Friction and Surface-Pressure Fluctuations on a Slender Wing at Incidence. R.A.E. Tech. Note Aero.2916. A.R.C.25 436. September, 1963.

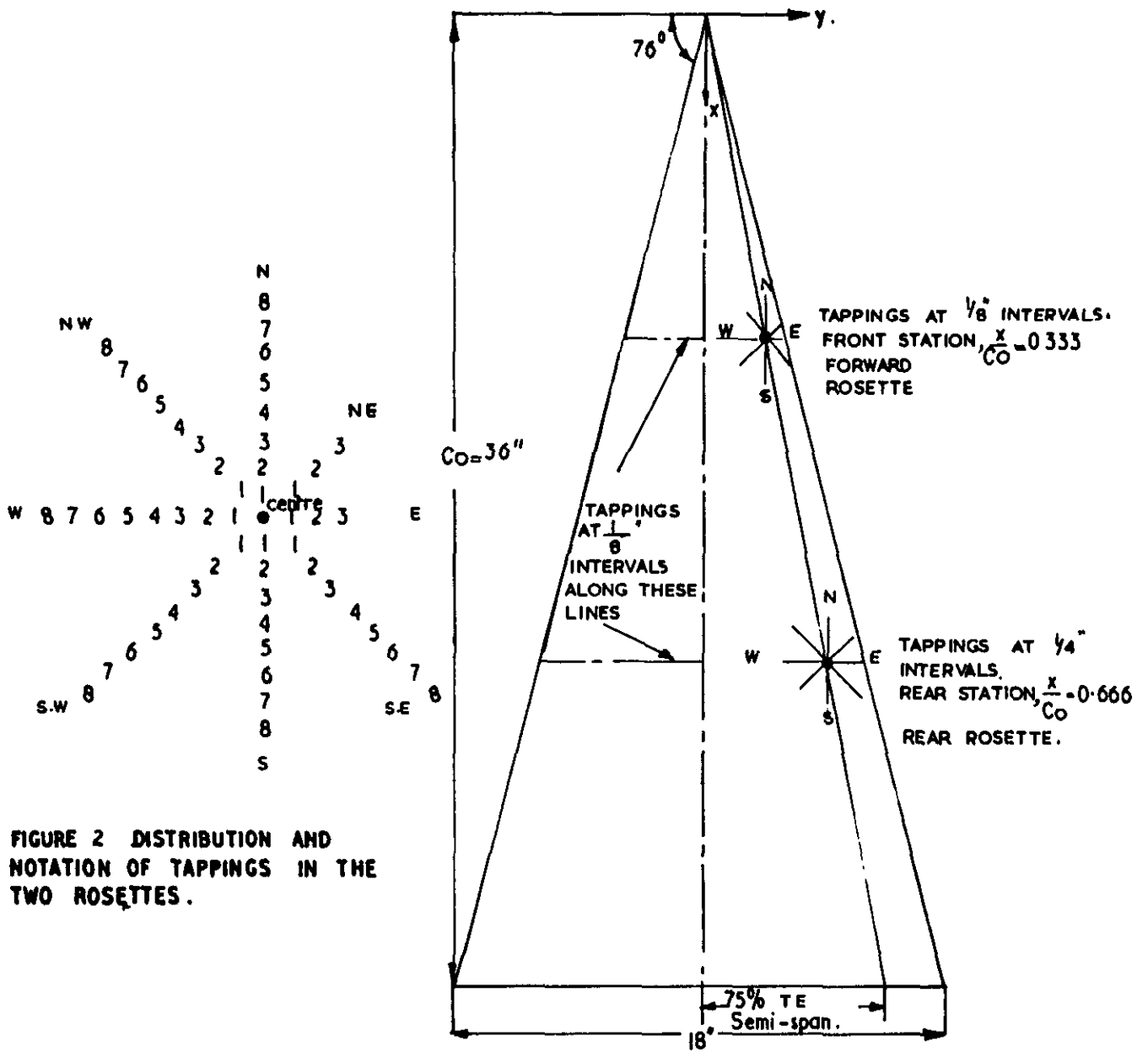


FIGURE 2 DISTRIBUTION AND NOTATION OF TAPPINGS IN THE TWO ROSETTES.

FIGURE 1. MODEL SHOWING DISTRIBUTION OF SURFACE PRESSURE TAPPINGS.

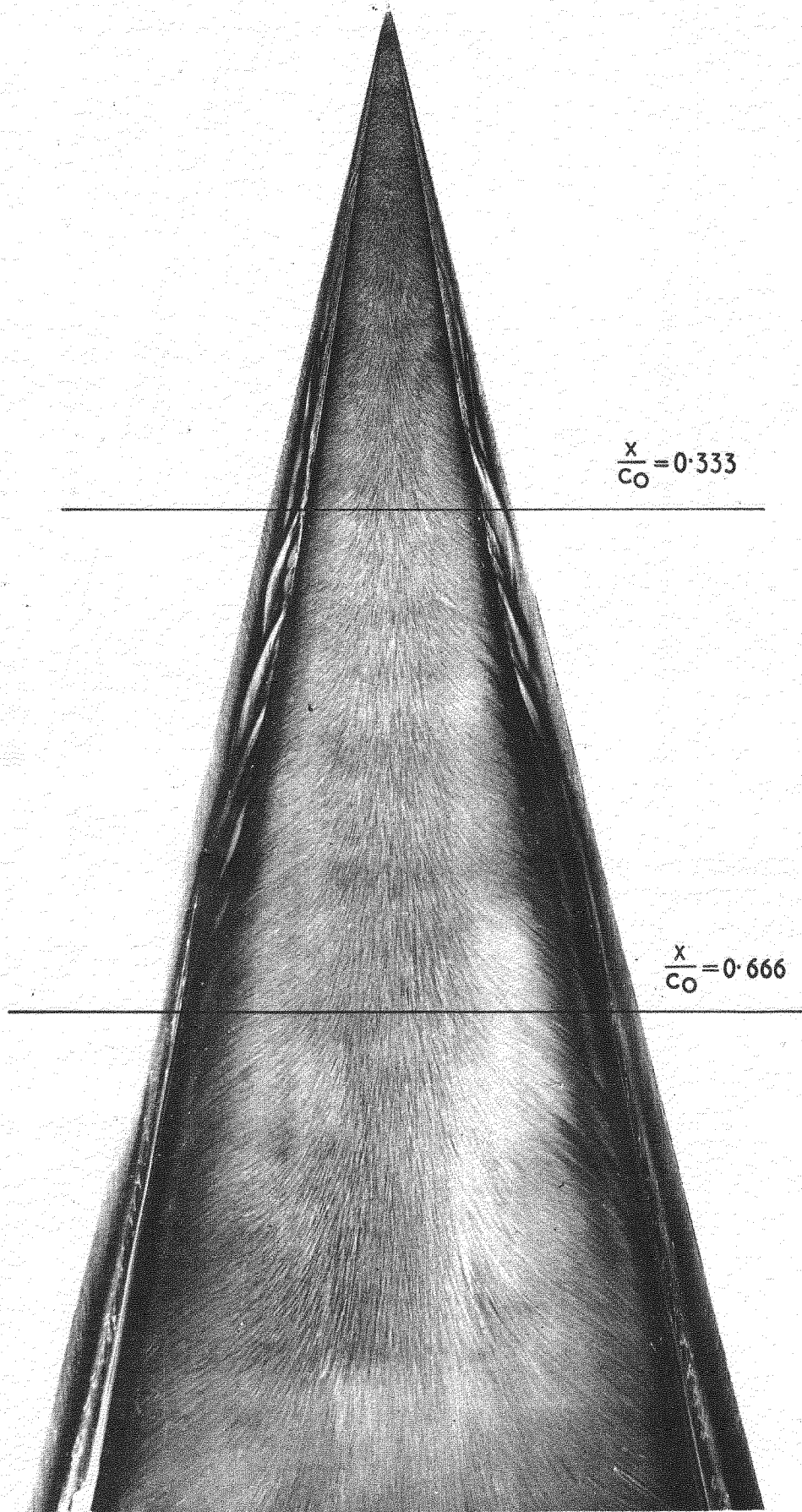


FIGURE 3. SURFACE FLOW PATTERN WITHOUT ROUGHNESS.  $\alpha = 15.5^\circ$

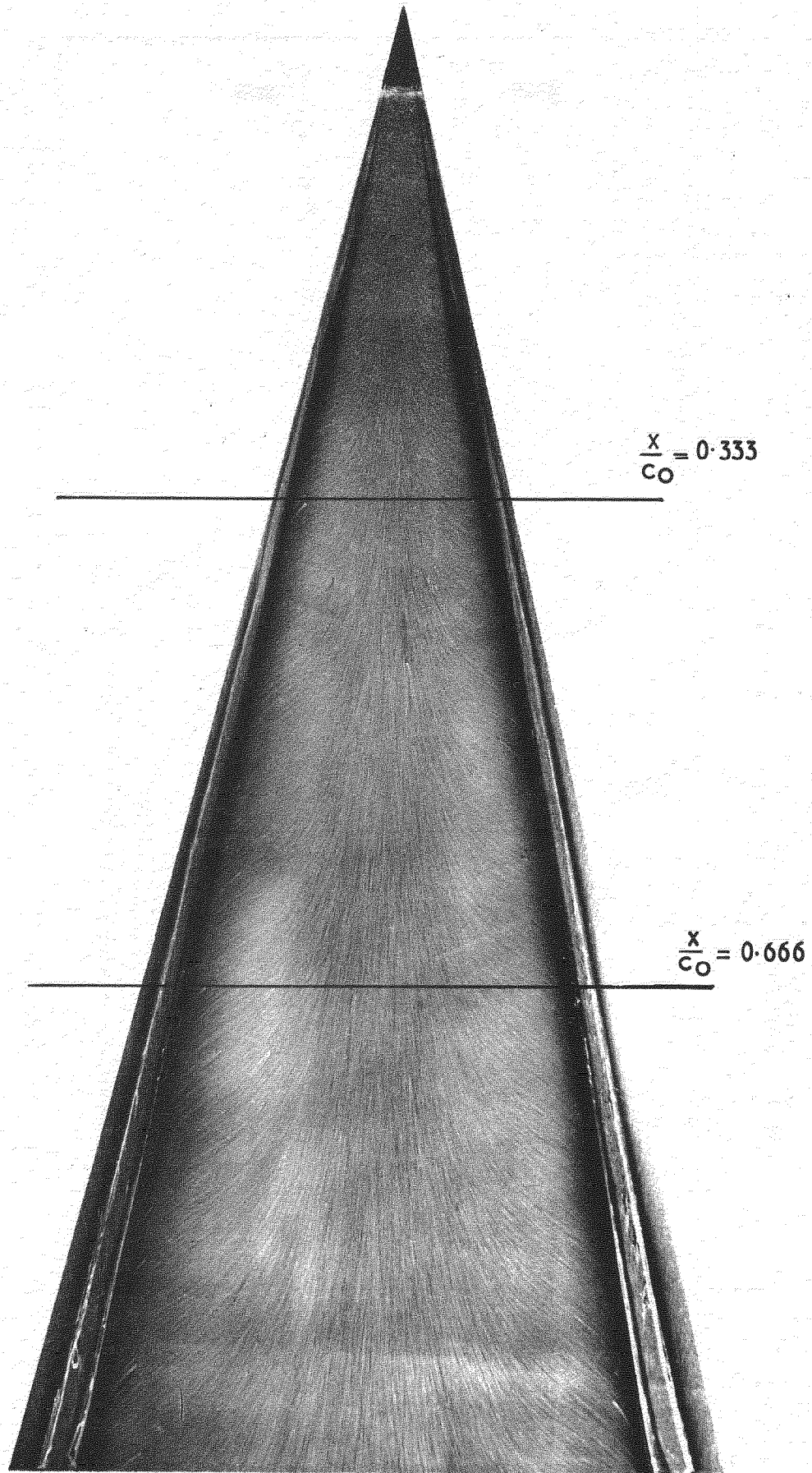


FIGURE 4. SURFACE FLOW PATTERN WITH ROUGHNESS AT THE APEX  $\alpha = 15.5^\circ$ .

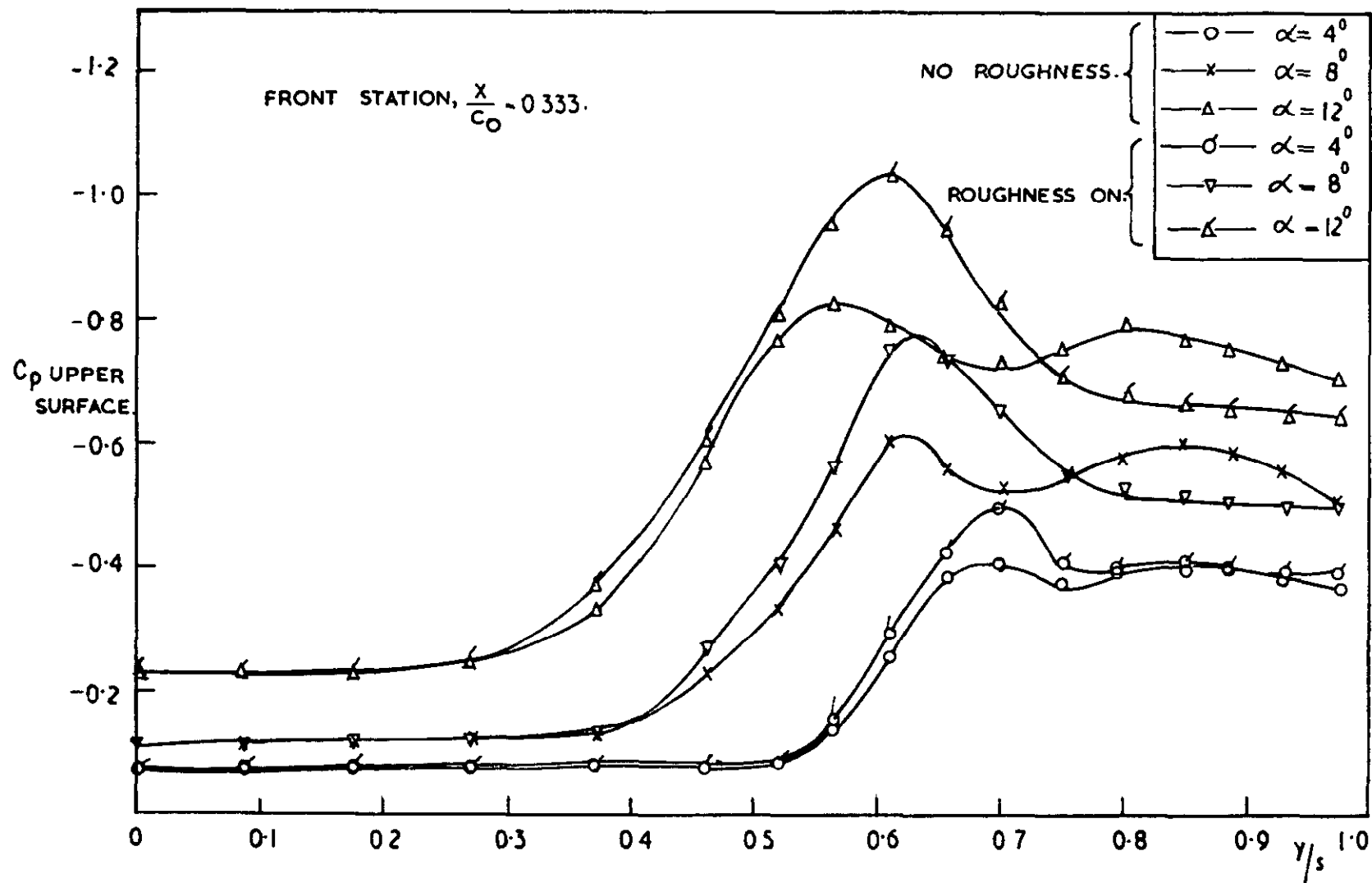


FIGURE 5 EFFECT OF SURFACE ROUGHNESS ON SPANWISE STATIC PRESSURE DISTRIBUTION.

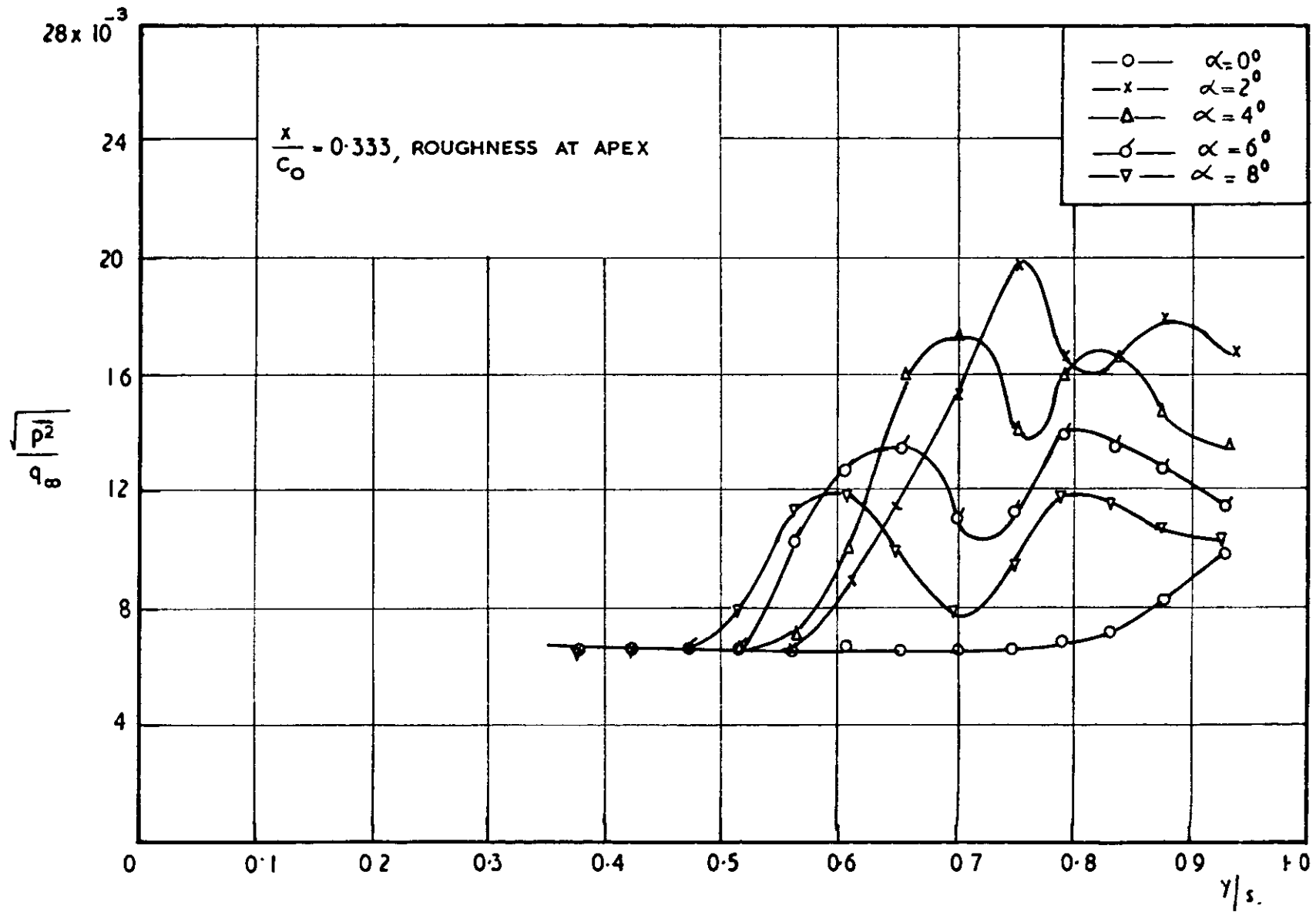


FIGURE 6 VARIATION OF R.M.S. PRESSURE FLUCTUATION WITH INCIDENCE AT THE FRONT STATION.

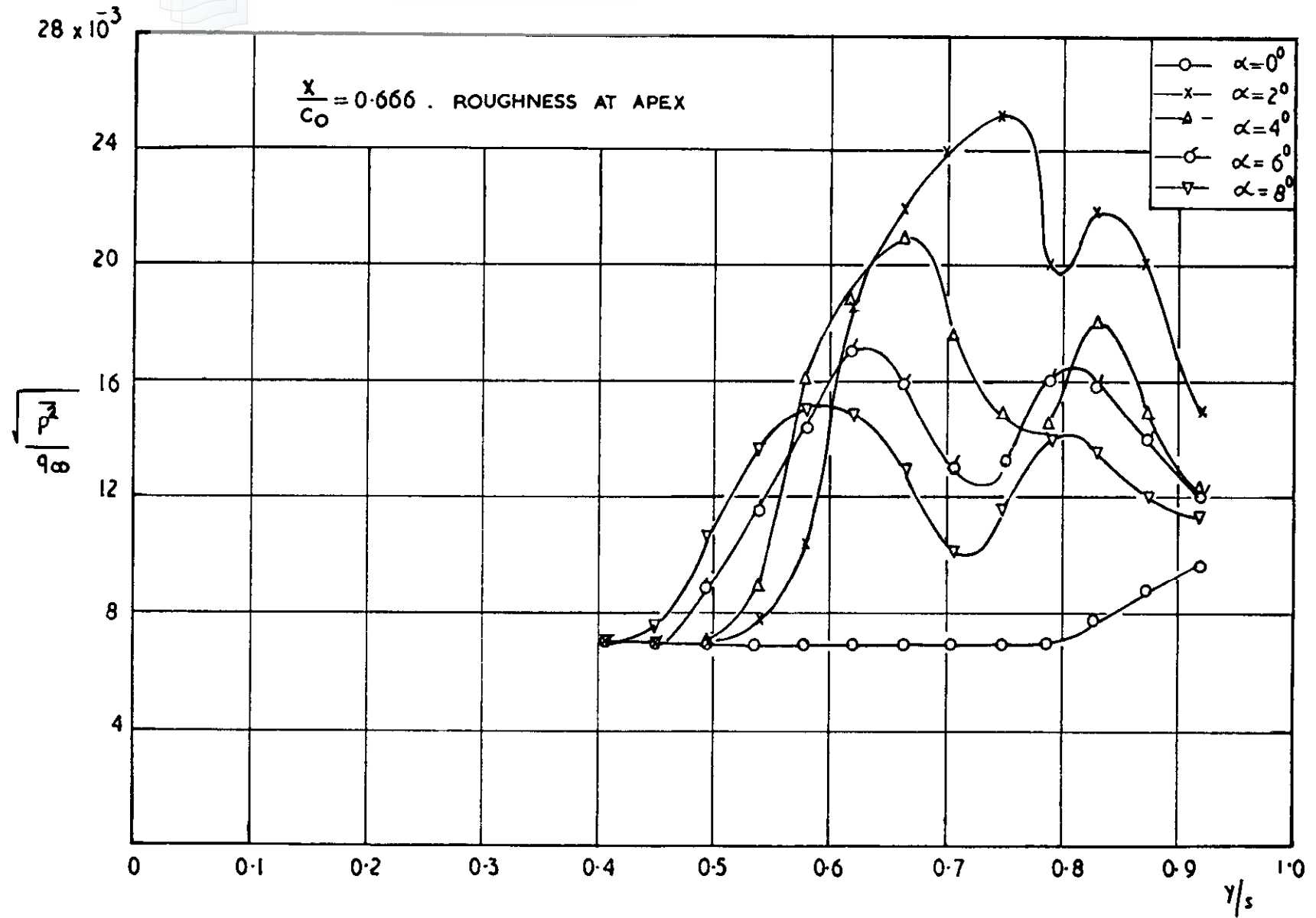


FIGURE 7 VARIATION OF R.M.S. PRESSURE FLUCTUATION WITH INCIDENCE AT THE REAR STATION .

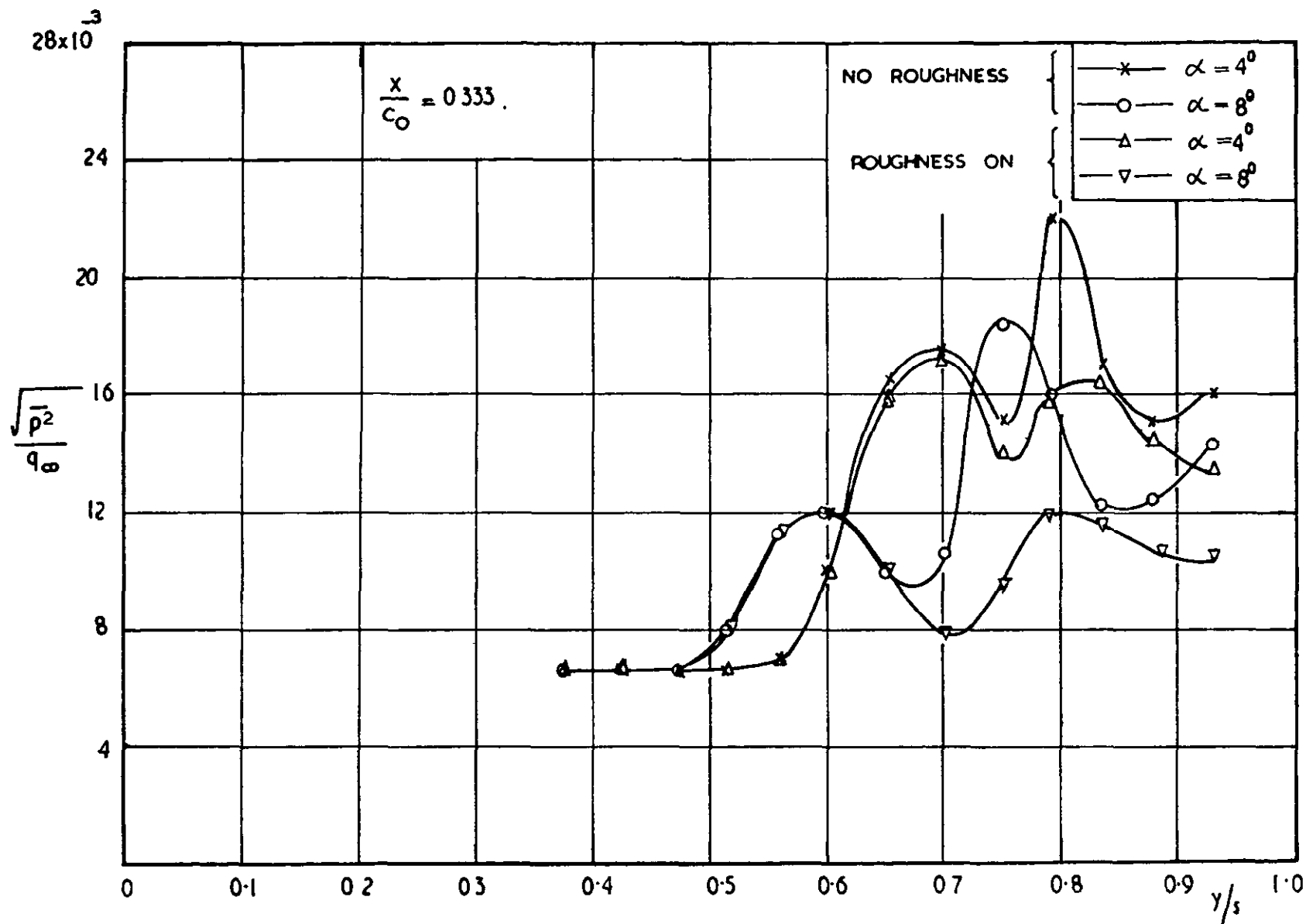


FIGURE 8. EFFECT OF ROUGHNESS ON THE R.M.S. PRESSURE FLUCTUATION AT THE FRONT STATION.

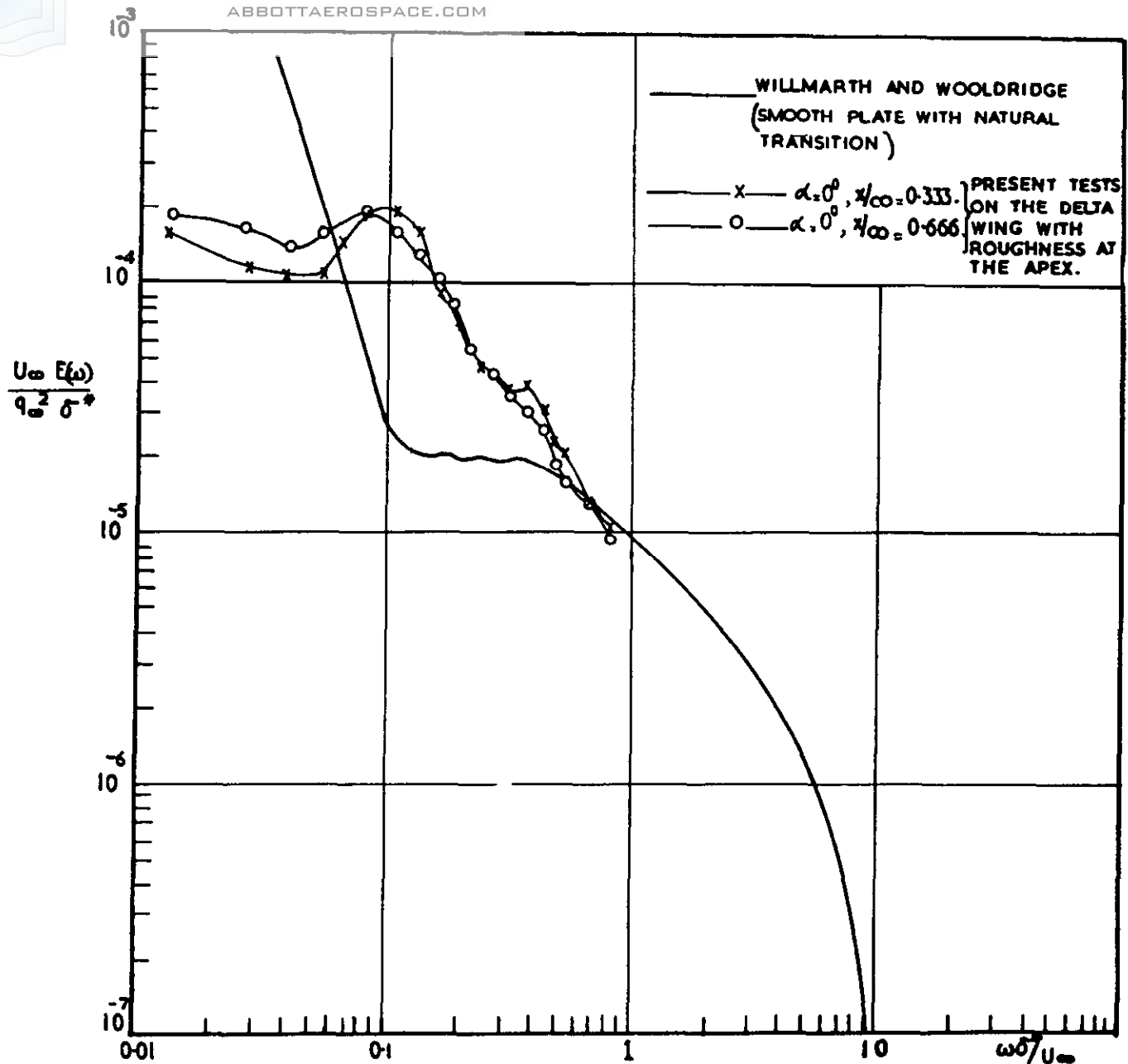


FIGURE 9. COMPARISON OF THE DIMENSIONLESS POWER SPECTRUM OF THE WALL PRESSURE WITH THOSE OF THE DELTA WING AT  $0^\circ$  INCIDENCE.

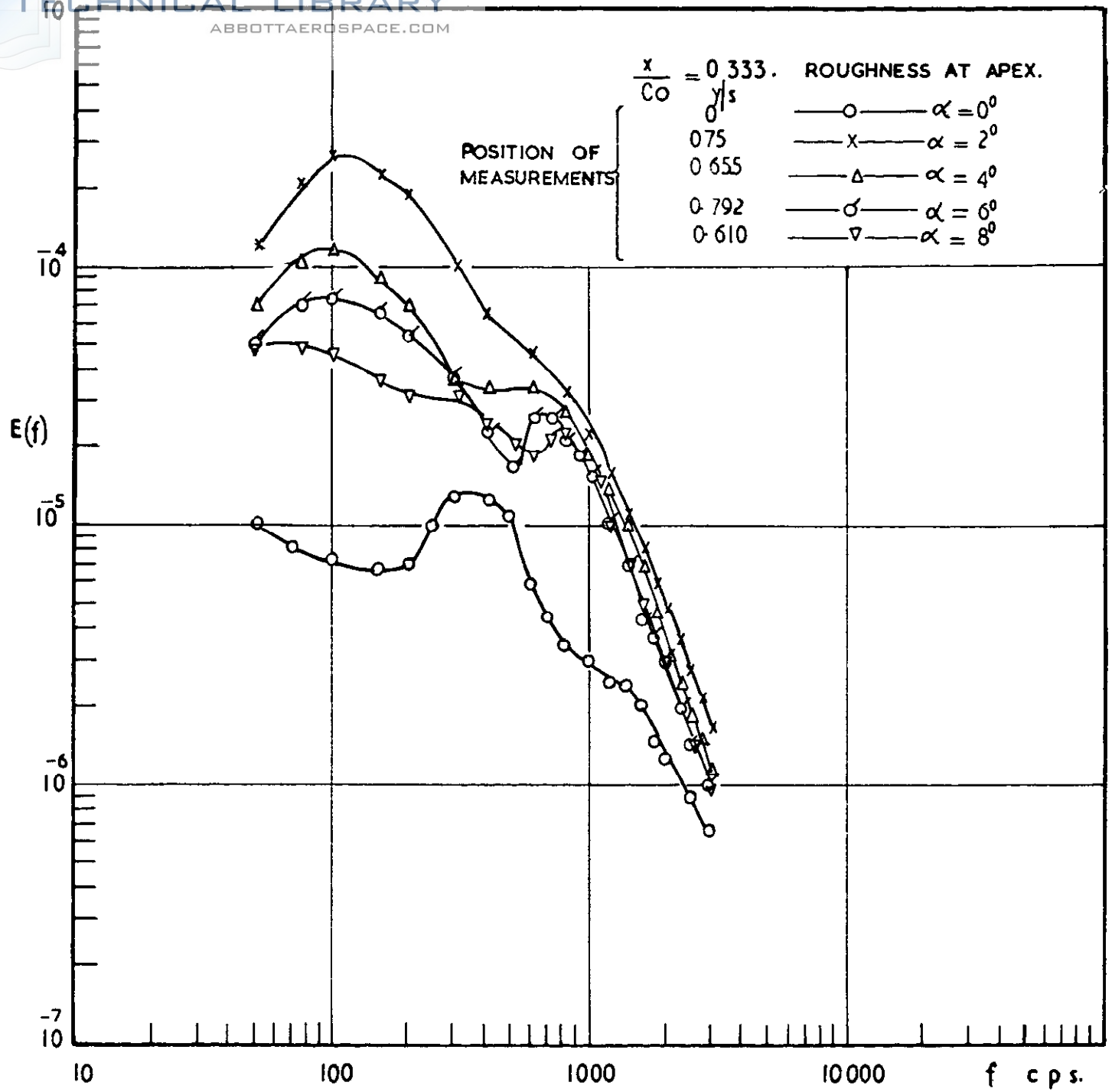


FIGURE 10. POWER SPECTRA OF PRESSURE FLUCTUATIONS AT THE FRONT STATION.

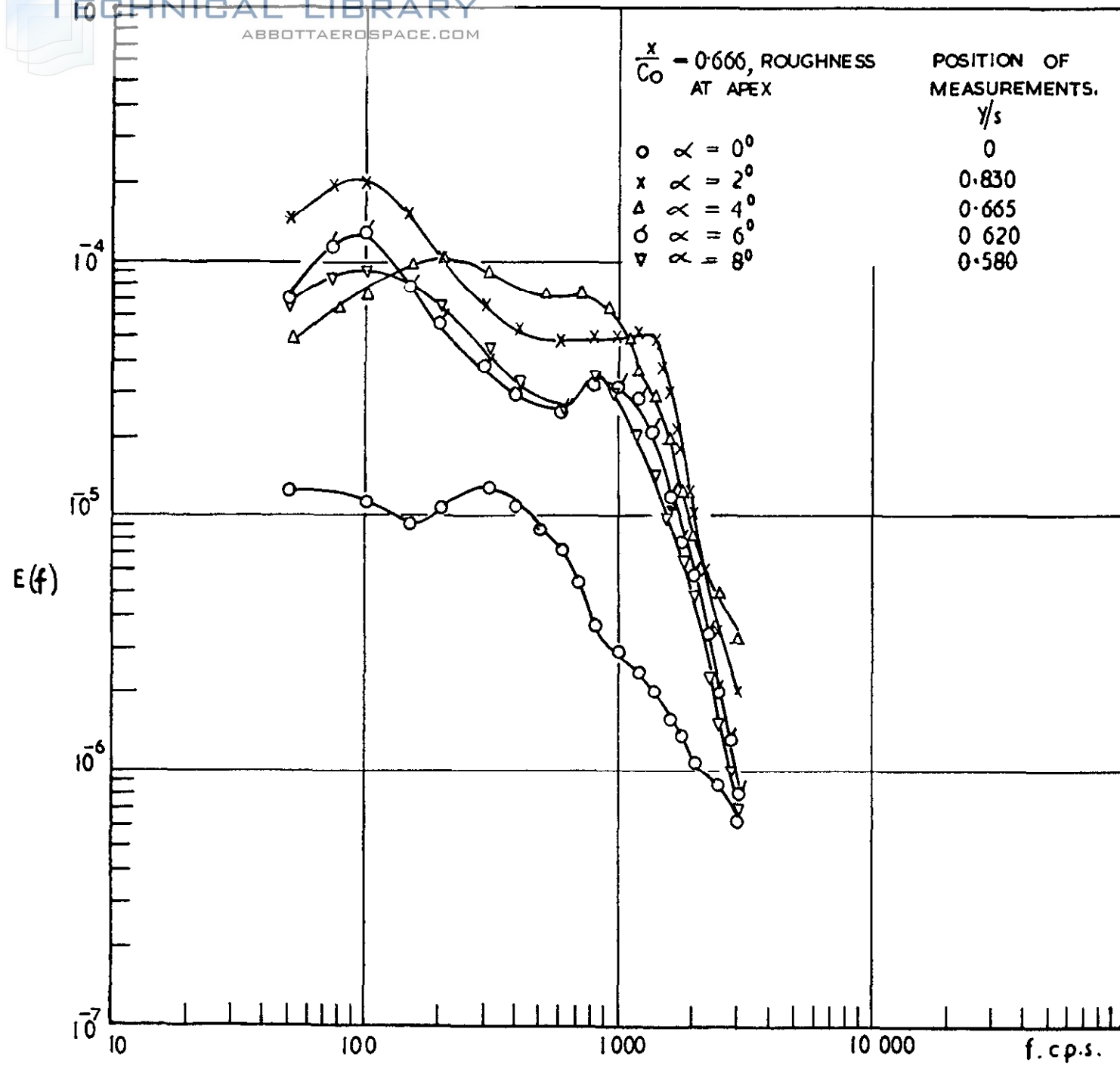
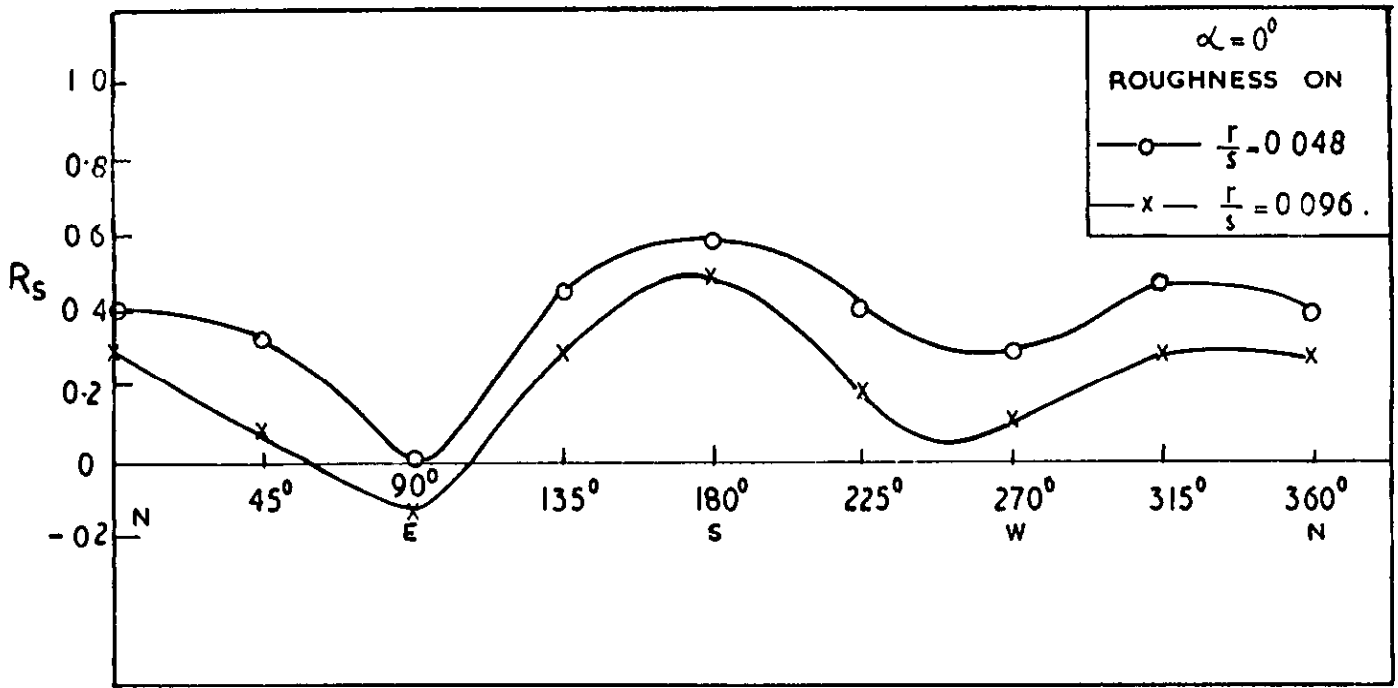
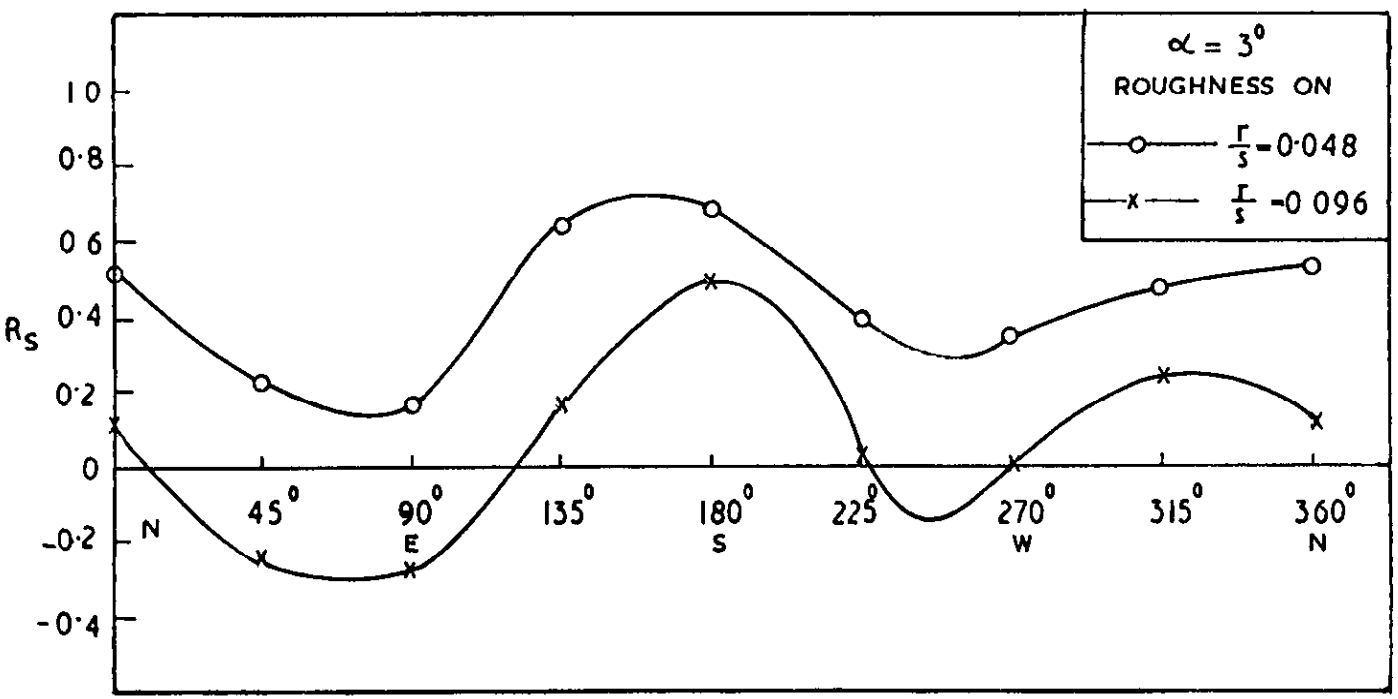


FIGURE II. POWER SPECTRA OF PRESSURE FLUCTUATIONS AT THE REAR STATION.

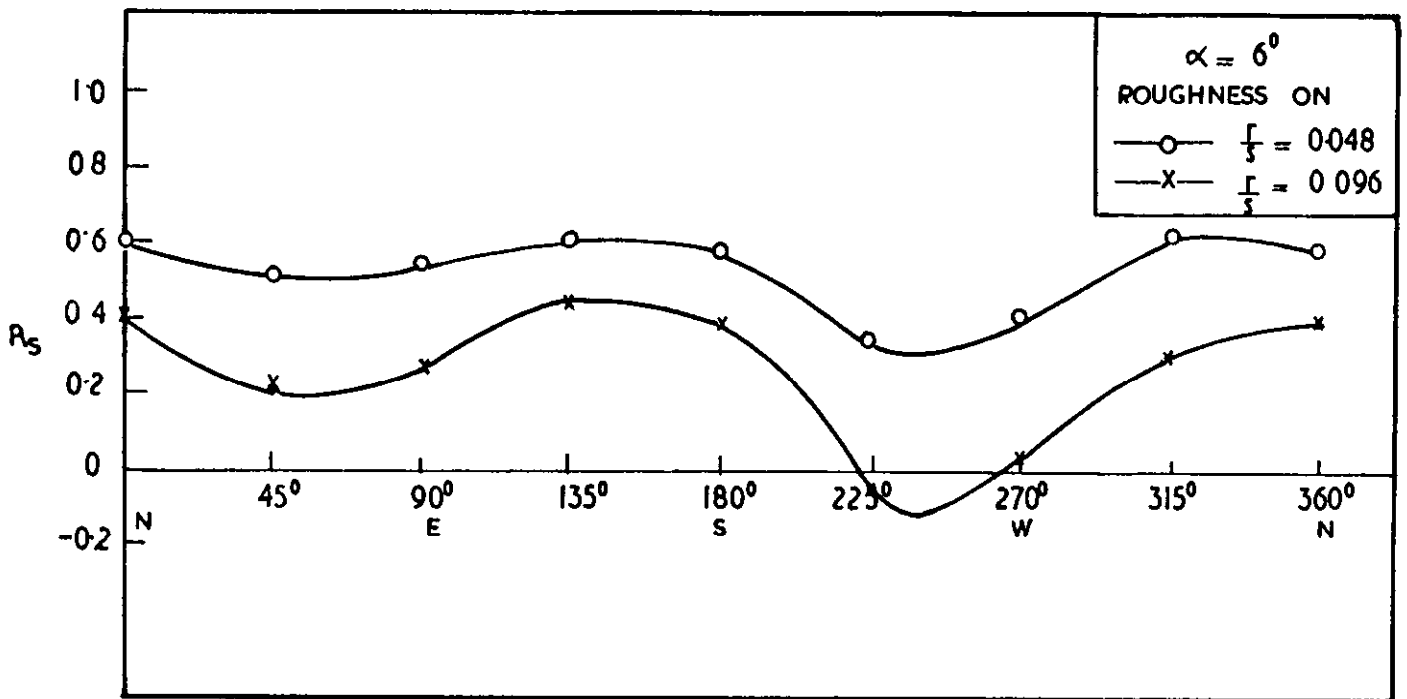


(a)

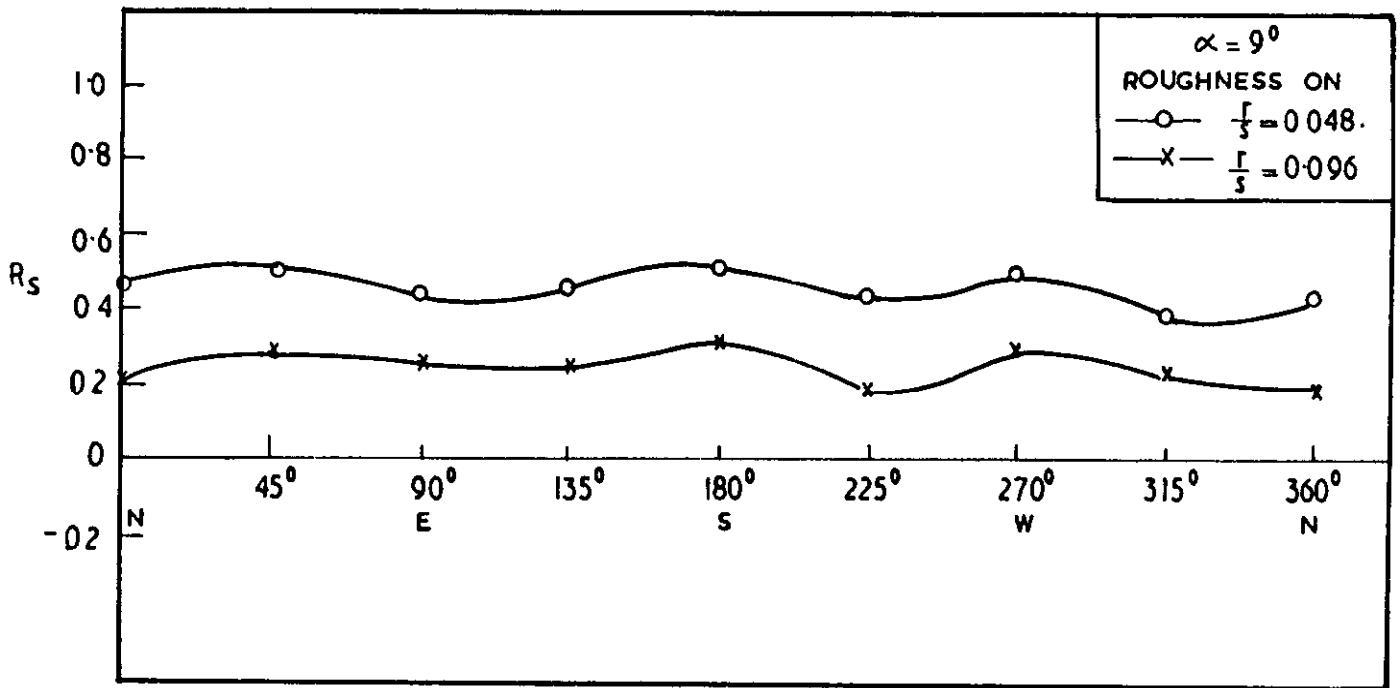


(b)

FIGURE 12 (a) (b)(c)(d) DIRECTIONAL VARIATION OF SPACE CORRELATION COEFFICIENT IN THE FORWARD ROSETTE.

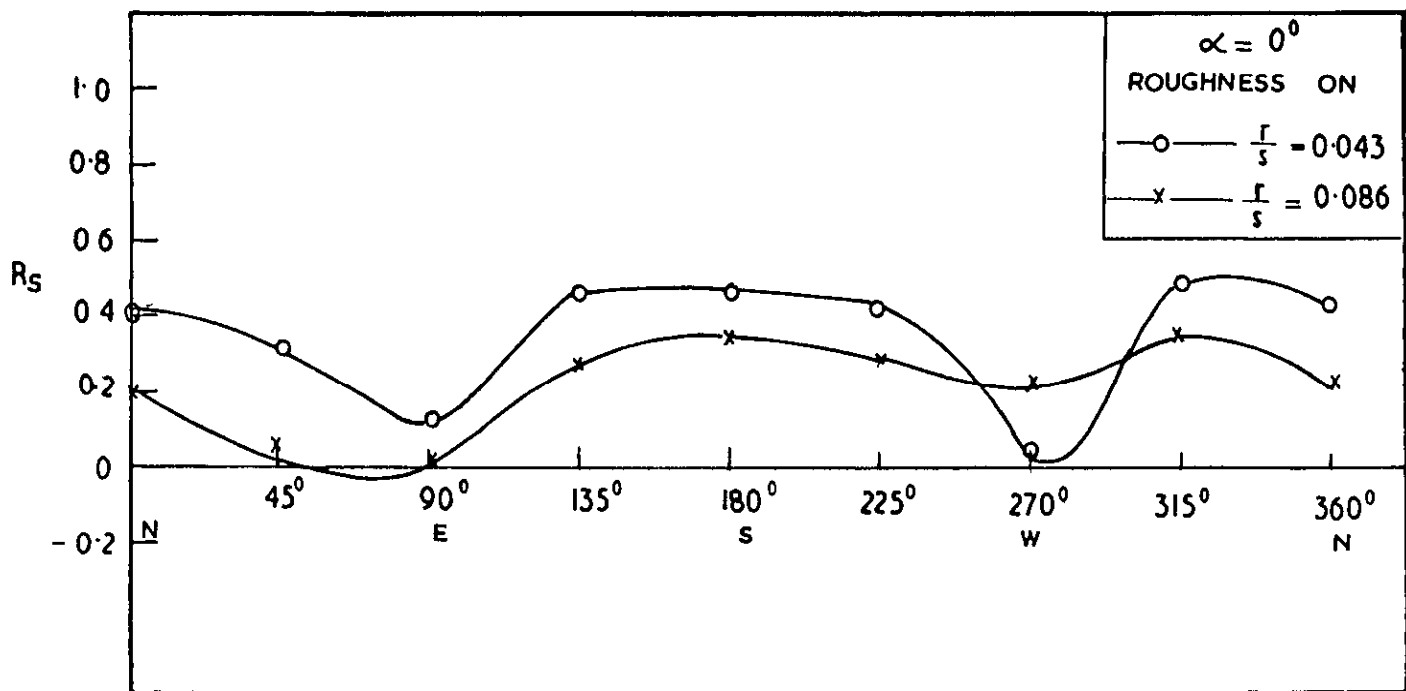


(c)

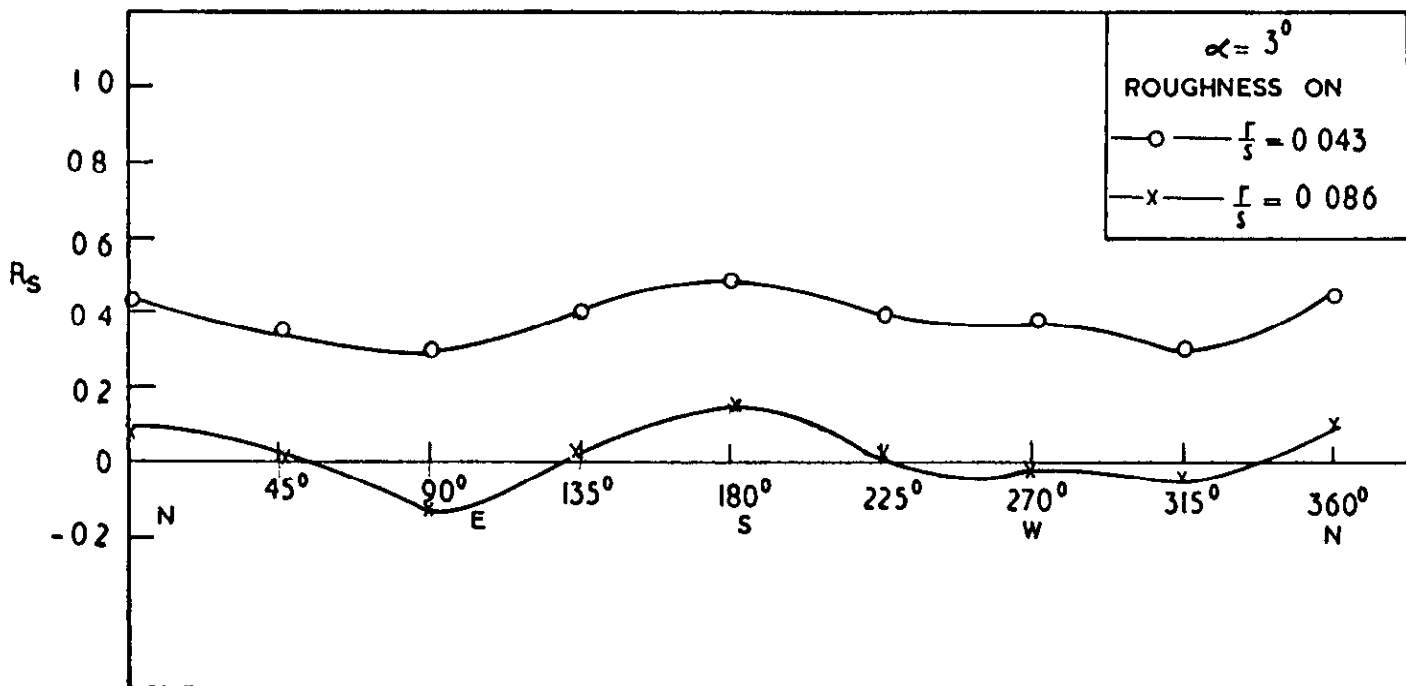


(d)

FIGURE 12. continued (c) and (d)

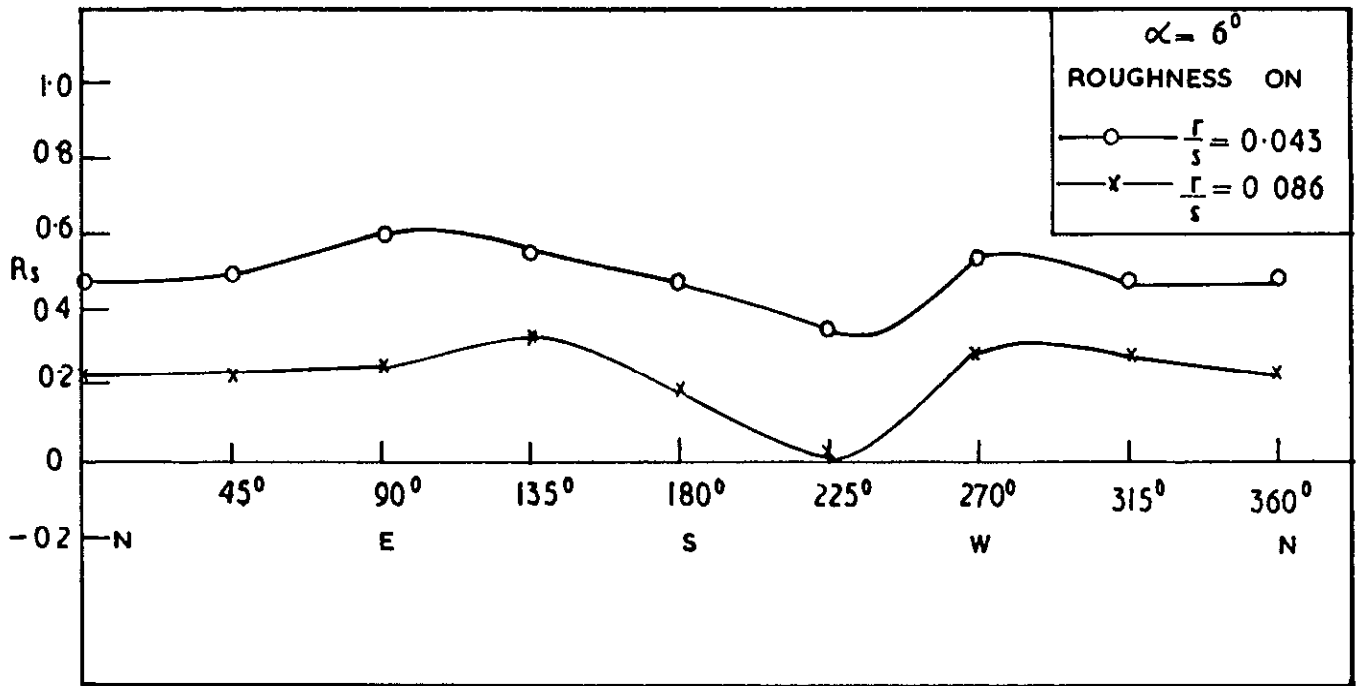


(a)

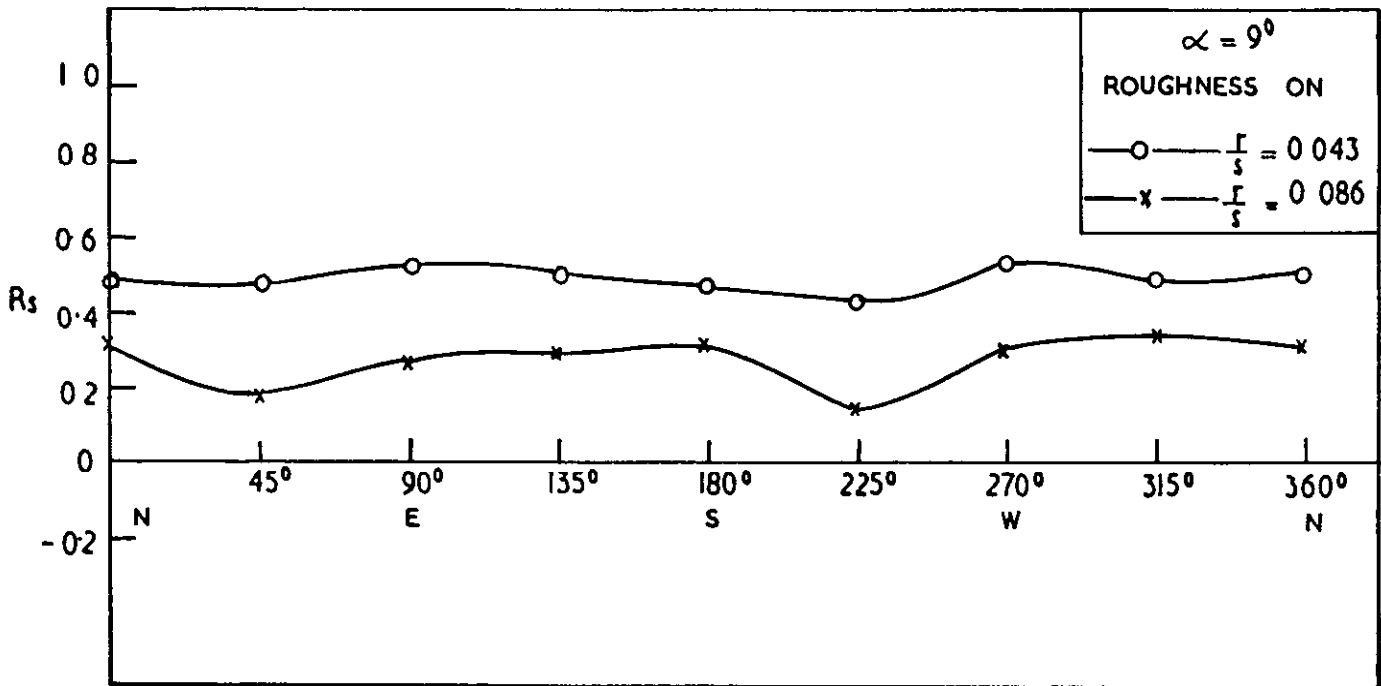


(b)

FIGURE 13 (a) (b) (c) (d) DIRECTIONAL VARIATION OF SPACE CORRELATION COEFFICIENT IN THE REAR ROSETTE.



(c.)



(d.)

FIGURE 13 (c) and (d)(continued)

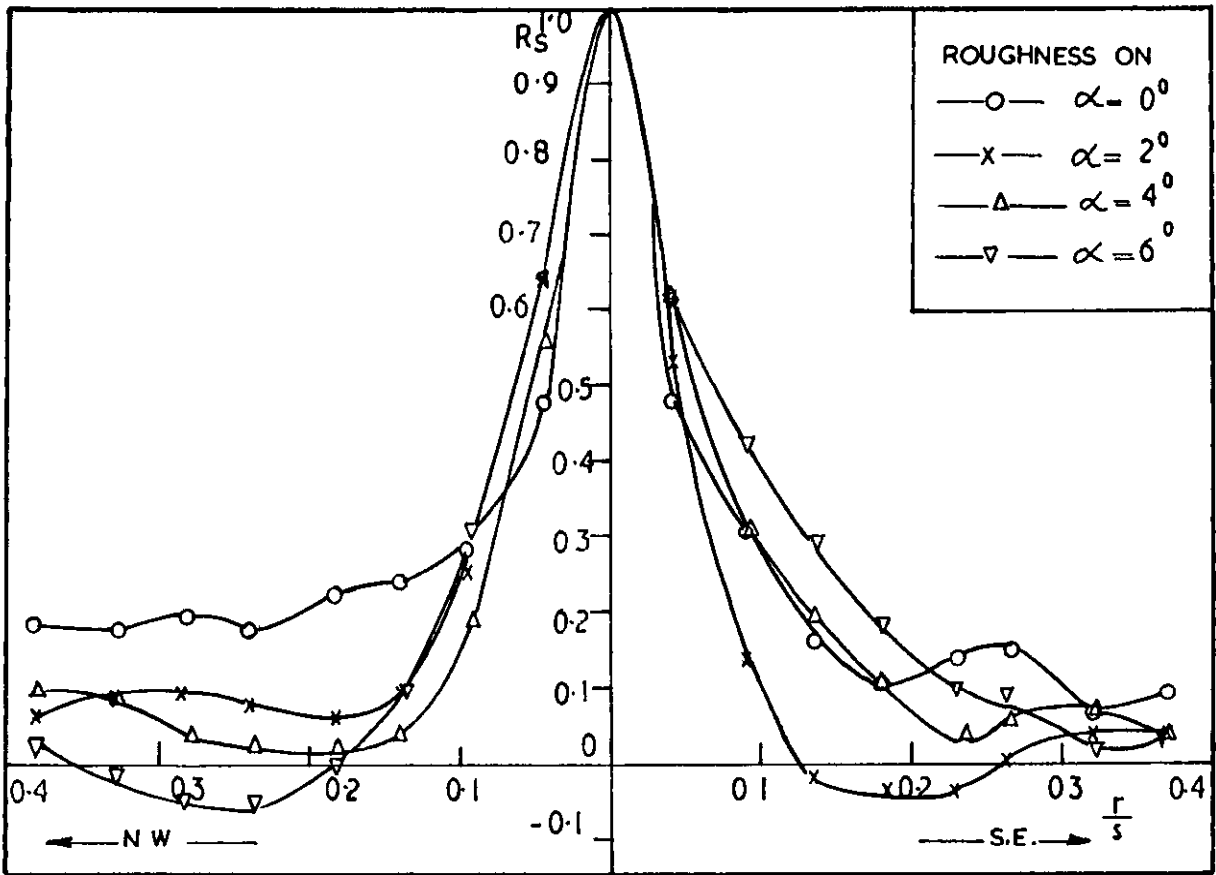


FIGURE 14. VARIATION OF SPACE CORRELATION COEFFICIENT ALONG N.W.-S.E. DIAGONAL OF FORWARD ROSETTE.

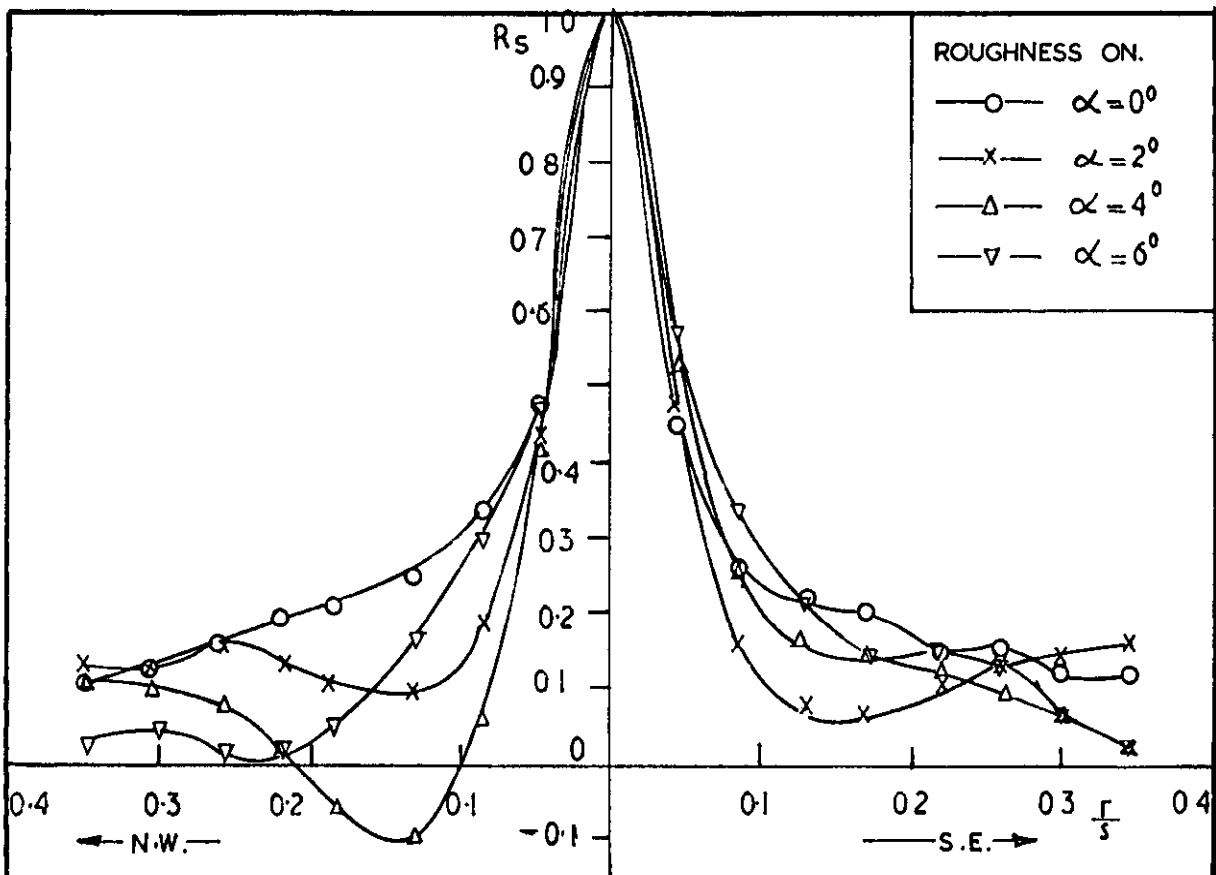
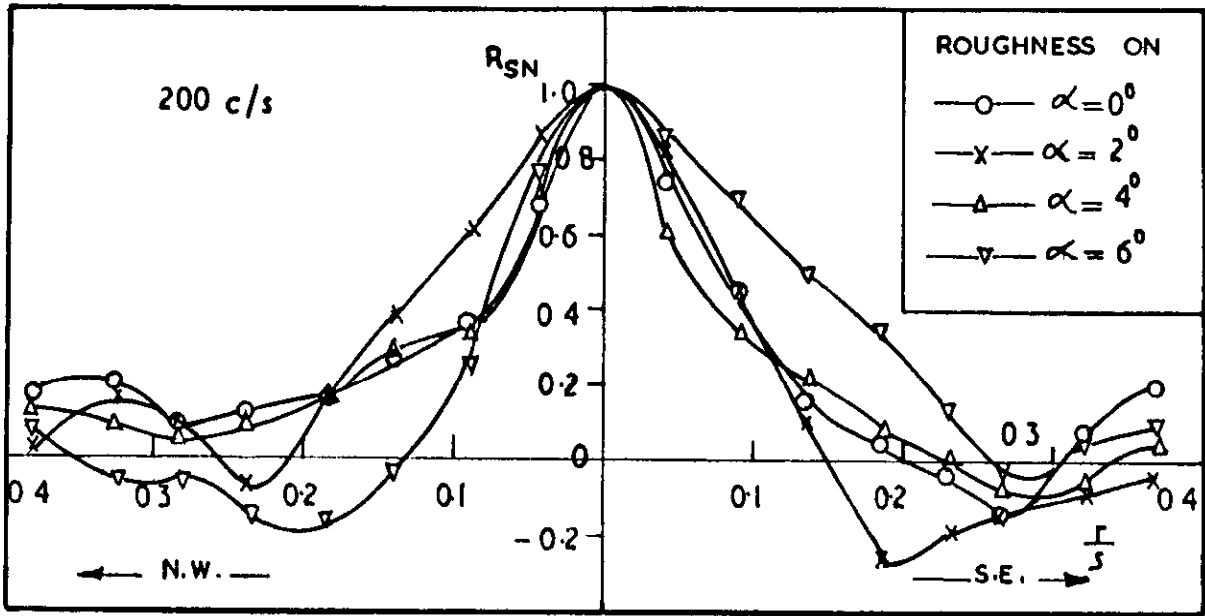
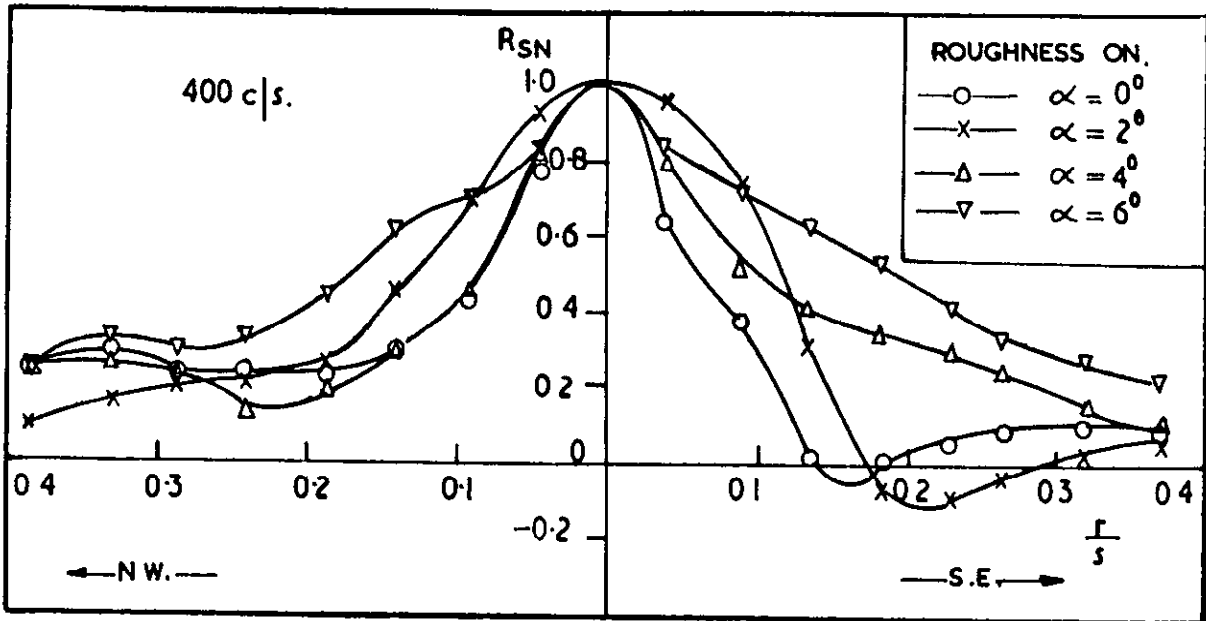


FIGURE 15 VARIATION OF SPACE CORRELATION COEFFICIENT ALONG N.W.-S.E. DIAGONAL OF REAR ROSETTE.

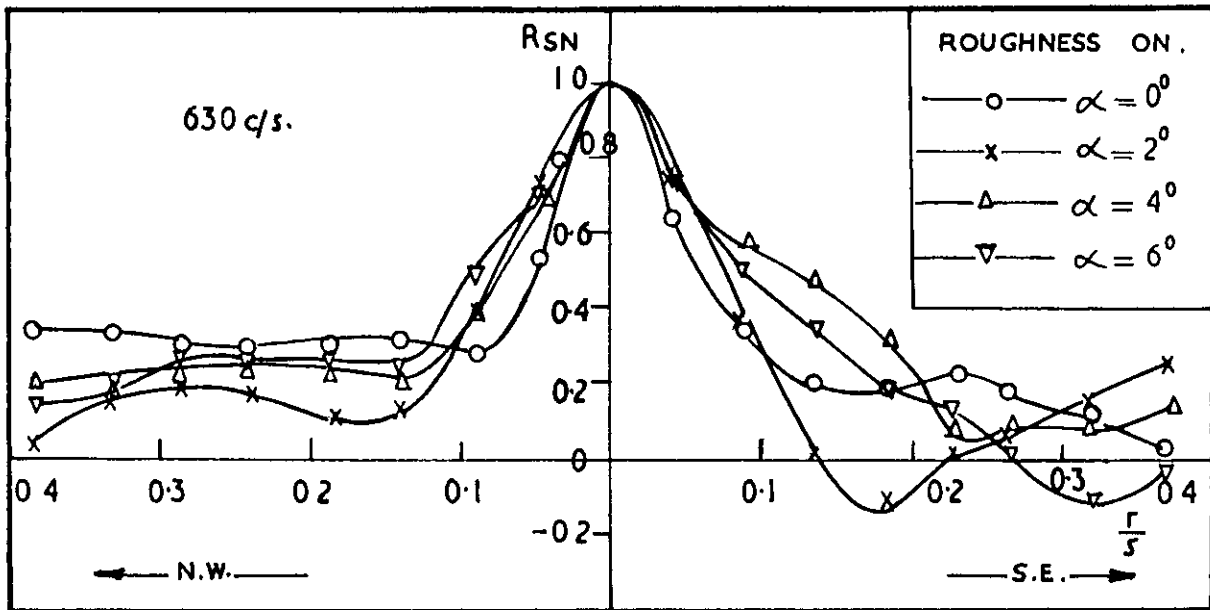


(a)

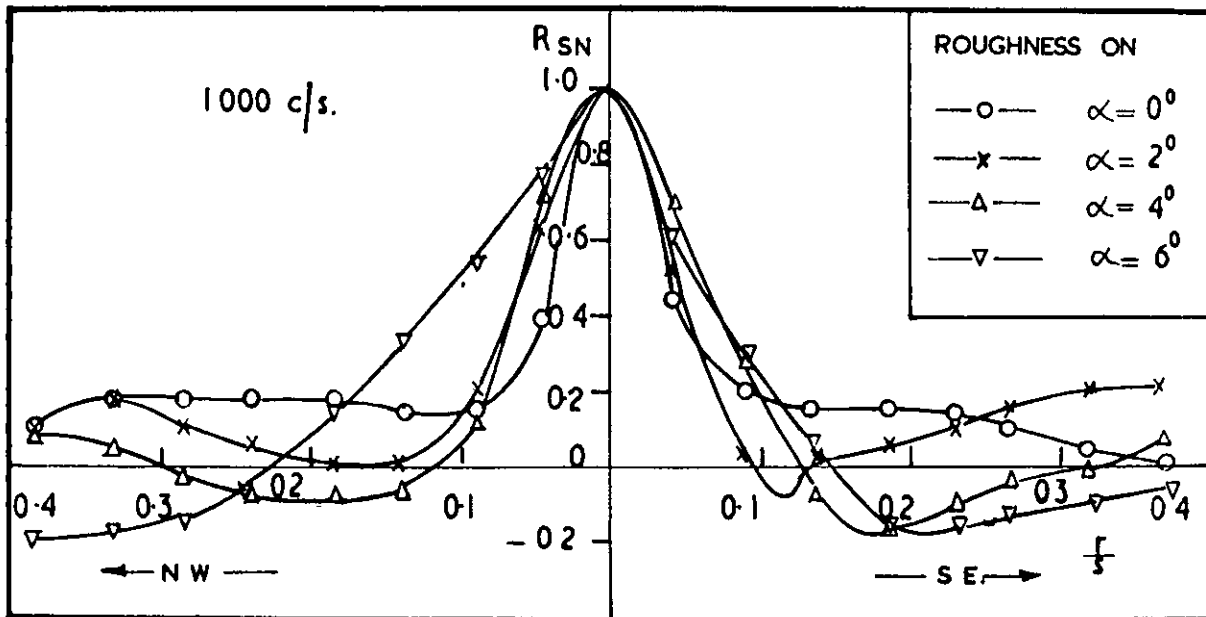


(b)

FIGURE 16. (a) (b) (c) (d) VARIATION OF SPACE CORRELATION COEFFICIENT ALONG N.W.-S.E. DIAGONAL OF FORWARD ROSETTE IN VARIOUS FREQUENCY BANDS.

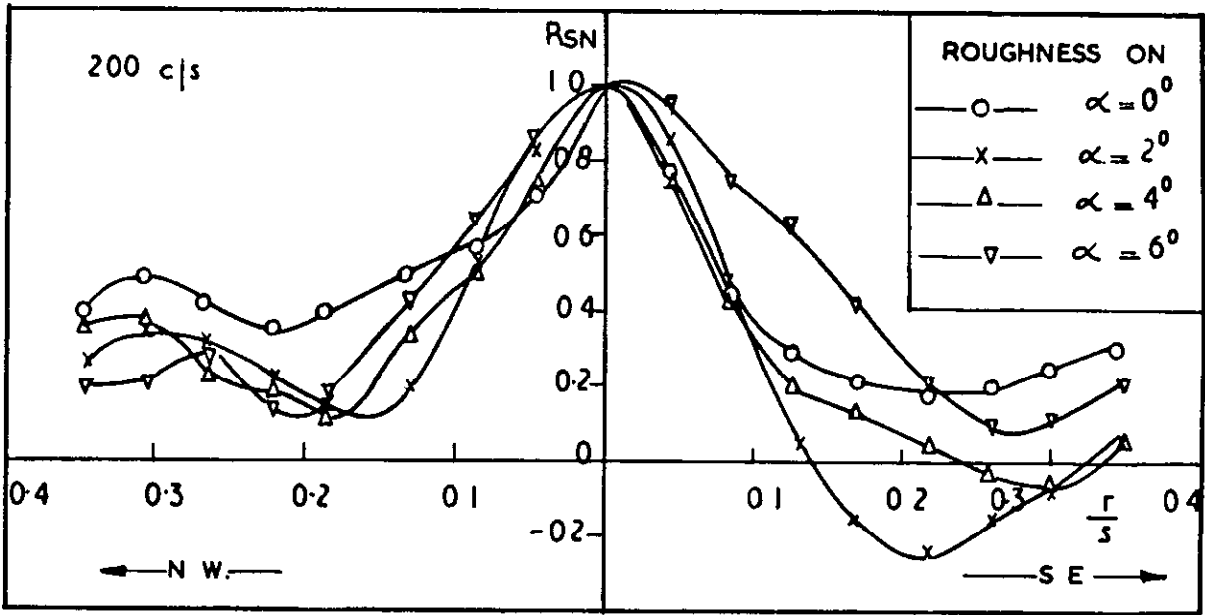


(c)

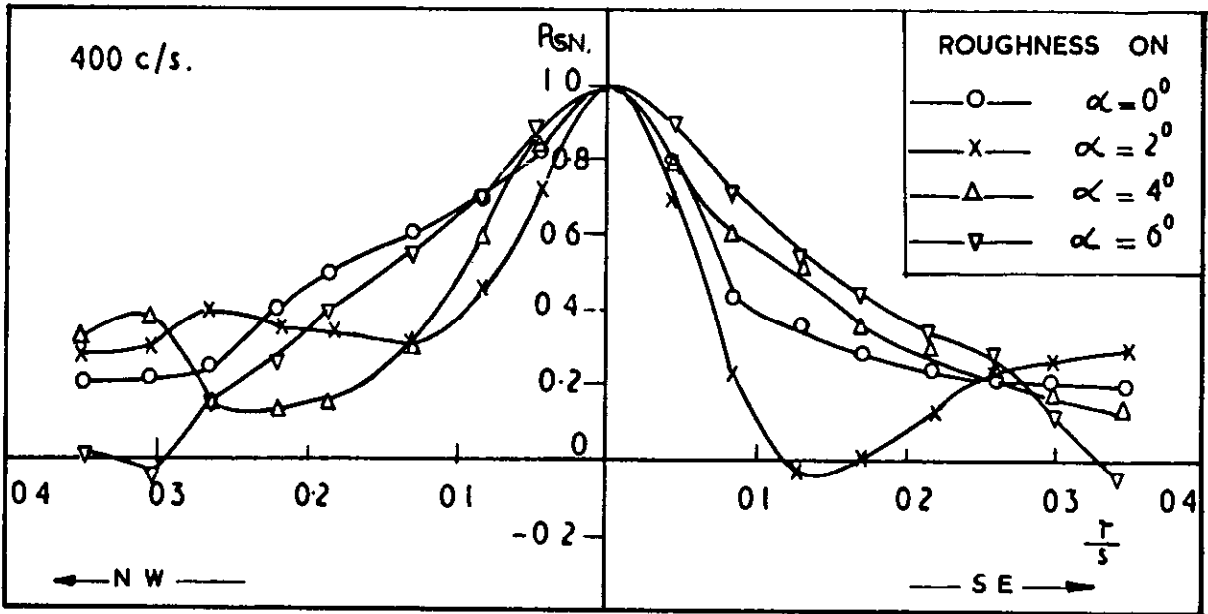


(d)

FIGURE 16 continued (c) and (d.)

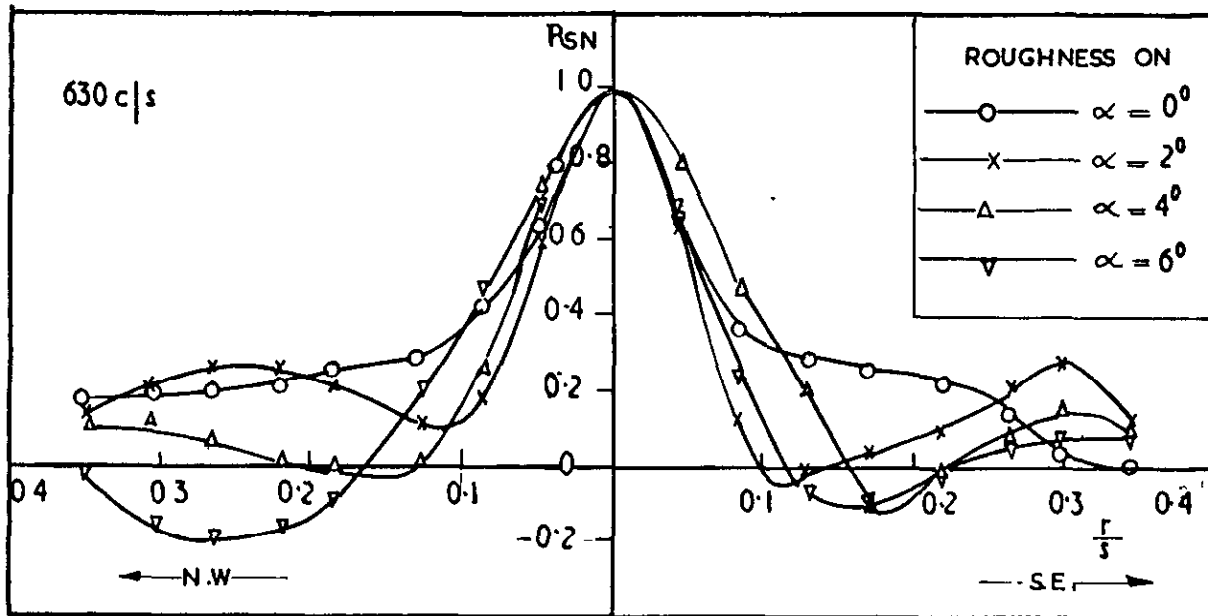


(a.)

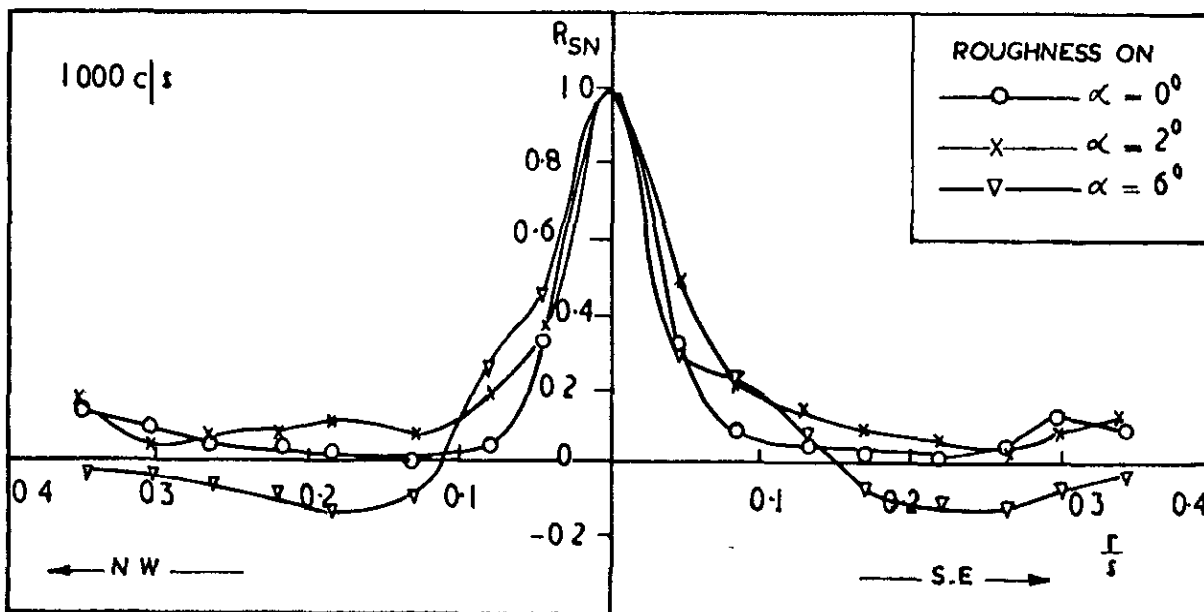


(b.)

FIGURE 17 (a)(b)(c)(d) VARIATION OF SPACE CORRELATION COEFFICIENT OF REAR ROSETTE IN VARIOUS FREQUENCY BANDS.



(c.)



(d.)

FIGURE 17 continued (c) and (d)

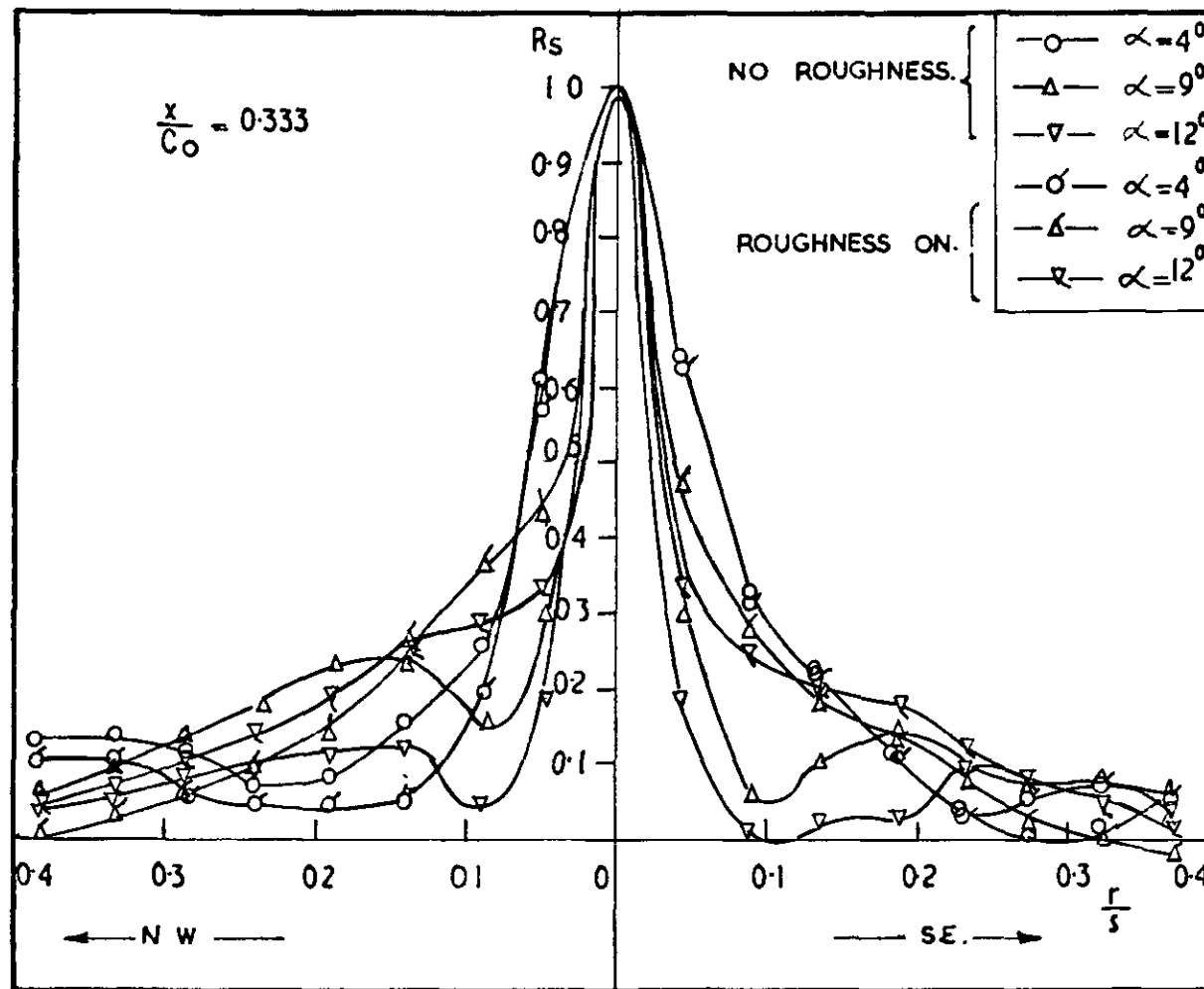


FIGURE 18 EFFECT OF ROUGHNESS ON THE SPACE CORRELATION COEFFICIENT ALONG THE N.W.-S.E. DIAGONAL OF FORWARD ROSETTE.

D 37988/1/Mc.60 K4 6/65 XL

A.R.C. C.P. No.767  
August, 1963  
V. Krishnamoorthy

MEASUREMENTS OF PRESSURE FLUCTUATIONS  
ON THE SURFACE OF A DELTA WING

Measurements have been made of the r.m.s. levels, spectra and space correlations of the surface pressure fluctuations on a  $76^\circ$  sharp edged delta wing at low incidences. The peak r.m.s. value was found to be 3.7 times that for the  $0^\circ$  incidence and occurred under the main vortex at  $2^\circ$  incidence. The forms of the spectra were found to be not dissimilar to that for  $0^\circ$  incidence. This suggests that the fluctuations arise from the boundary layer modified by the vortex. The correlation radius was found to be about  $\frac{1}{15}$  th of the local semi-span. However, correlation lengths for discrete frequencies could be twice as large as this.

A.R.C. C.P. No.767  
August, 1963  
V. Krishnamoorthy

MEASUREMENTS OF PRESSURE FLUCTUATIONS  
ON THE SURFACE OF A DELTA WING

Measurements have been made of the r.m.s. levels, spectra and space correlations of the surface pressure fluctuations on a  $76^\circ$  sharp edged delta wing at low incidences. The peak r.m.s. value was found to be 3.7 times that for the  $0^\circ$  incidence and occurred under the main vortex at  $2^\circ$  incidence. The forms of the spectra were found to be not dissimilar to that for  $0^\circ$  incidence. This suggests that the fluctuations arise from the boundary layer modified by the vortex. The correlation radius was found to be about  $\frac{1}{15}$  th of the local semi-span. However, correlation lengths for discrete frequencies could be twice as large as this.

A.R.C. C.P. No.767  
August, 1963  
V. Krishnamoorthy

MEASUREMENTS OF PRESSURE FLUCTUATIONS  
ON THE SURFACE OF A DELTA WING

Measurements have been made of the r.m.s. levels, spectra and space correlations of the surface pressure fluctuations on a  $76^\circ$  sharp edged delta wing at low incidences. The peak r.m.s. value was found to be 3.7 times that for the  $0^\circ$  incidence and occurred under the main vortex at  $2^\circ$  incidence. The forms of the spectra were found to be not dissimilar to that for  $0^\circ$  incidence. This suggests that the fluctuations arise from the boundary layer modified by the vortex. The correlation radius was found to be about  $\frac{1}{15}$  th of the local semi-span. However, correlation lengths for discrete frequencies could be twice as large as this.

DETACHABLE ABSTRACT CARDS





**C.P. No. 767**

© *Crown copyright 1965*

Printed and published by

**HER MAJESTY'S STATIONERY OFFICE**

To be purchased from

**York House, Kingsway, London w c.2**

**423 Oxford Street, London w 1**

**13A Castle Street, Edinburgh 2**

**109 St. Mary Street, Cardiff**

**39 King Street, Manchester 2**

**50 Fairfax Street, Bristol 1**

**35 Smallbrook, Ringway, Birmingham 5**

**80 Chichester Street, Belfast 1**

or through any bookseller

*Printed in England*

**C.P. No. 767**

**S.O. Code No. 23-9015-67**